ENCAPSULATION OF CAFFEIC ACID IN CAROB BEAN FLOUR AND WHEY PROTEIN-BASED NANOFIBERS BY ELECTROSPINNING

A THESIS SUBMITTED TO
THE GRADUATE SCHOOL OF NATURAL AND APPLIED SCIENCES
OF
MIDDLE EAST TECHNICAL UNIVERSITY

BY

SEMA ZEREN

IN PARTIAL FULFILLMENT OF THE REQUIREMENTS
FOR
THE DEGREE OF MASTER OF SCIENCE
IN
FOOD ENGINEERING

NOVEMBER 2022

Approval of the thesis:

ENCAPSULATION OF CAFFEIC ACID IN CAROB BEAN FLOUR AND WHEY PROTEIN-BASED NANOFIBERS BY ELECTROSPINNING

submitted by **SEMA ZEREN** in partial fulfillment of the requirements for the degree of **Master of Science** in **Food Engineering, Middle East Technical University** by,

Prof. Dr. Halil Kalıpçılar
Dean, Graduate School of **Natural and Applied Sciences** _____

Prof. Dr. Hami Alpas
Head of the Department, **Food Engineering** _____

Prof. Dr. Serpil Şahin
Supervisor, **Food Engineering, METU** _____

Prof. Dr. Gülüm Şumnu
Co-Supervisor, **Food Engineering, METU** _____

Examining Committee Members:

Prof. Dr. Hami Alpas
Food Engineering, METU _____

Prof. Dr. Serpil Şahin
Food Engineering, METU _____

Prof. Dr. Gülüm Şumnu
Food Engineering, METU _____

Assist. Prof. Dr. Leyla Nesrin Kahyaoğlu
Food Engineering, METU _____

Assist. Prof. Dr. Ayça Aydoğdu Emir
Food Technology, Canakkale 18 Mart Un. _____

Date:

I hereby declare that all information in this document has been obtained and presented in accordance with academic rules and ethical conduct. I also declare that, as required by these rules and conduct, I have fully cited and referenced all material and results that are not original to this work.

Name Last name : Sema Zeren

Signature :

ABSTRACT

ENCAPSULATION OF CAFFEIC ACID IN CAROB BEAN FLOUR AND WHEY PROTEIN-BASED NANOFIBERS BY ELECTROSPINNING

Zeren, Sema
Master of Science, Food Engineering
Supervisor : Prof. Dr. Serpil Şahin
Co-Supervisor: Prof. Dr. Gülüm Şumnu

November 2022, 69 pages

The purpose of this study was to introduce caffeic acid (CA) into electrospun nanofibers made of carob flour, whey protein concentrate (WPC), and polyethylene oxide (PEO). The effects of WPC concentration (1% and 3%) and CA additions (1% and 10%) on the characteristics of solutions and nanofibers were investigated. The viscosity and electrical conductivity of the solutions were examined to determine characteristics of solutions. Scanning electron microscopy (SEM), X-ray diffraction (XRD), thermogravimetric analyzer (TGA), differential scanning calorimetry (DSC), water vapor permeability (WVP), and Fourier transform infrared (FTIR) analysis were used to characterize the nanofibers. According to the SEM results, the inclusion of CA into nanofibers resulted in thinner nanofibers. All nanofibers exhibited uniform morphology. CA was efficiently loaded into nanofibers. The increase in CA concentrations from 1% to 10%, increased loading efficiencies from 76.4% to 94%. Nanofibers containing 10% CA demonstrated 92.95% antioxidant activity. The results indicated that encapsulating CA into carob flour/WPC-based nanofibers via electrospinning is a suitable candidate for active packaging applications.

Keywords: Active packaging, Biodegradable packaging, Electrospinning, Carob flour, Encapsulation

ÖZ

KAFEİK ASİTİN ELEKTROEĞİRME YÖNTEMİ İLE KEÇİBOYNUZU UNU VE PEYNİR ALTI SUYU PROTEİNİ İÇEREN NANOLİFLER İÇİNE HAPSEDİLMESİ

Zeren, Sema
Yüksek Lisans, Gıda Mühendisliği
Tez Yöneticisi: Prof. Dr. Serpil Şahin
Ortak Tez Yöneticisi: Prof. Dr. Gülüm Şumnu

Kasım 2022, 69 sayfa

Bu çalışmanın amacı, keçiboynuzu unu, peynir altı suyu proteini konsantresi ve polietilen oksitten (PEO) yapılan elektroeğrilmiş nanoliflere kafeik asit eklemektir. Peynir altı suyu proteini konsantresi konsantrasyonunun (%1 ve %3) ve kafeik asit ilavelerinin (%1 ve %10) çözeltilerin ve nanoliflerin özellikleri üzerindeki etkileri araştırılmıştır. Çözeltilerin özelliklerini belirlemek için çözeltilerin viskozitesi ve elektriksel iletkenliği incelenmiştir. Nanolifleri karakterize etmek için taramalı elektron mikroskobu (SEM), X-ışını kırınımı (XRD), termal gravimetrik analiz (TGA), diferansiyel taramalı kalorimetri (DSC), su buharı geçirgenliği (WVP) ve Fourier dönüşümü kızılötesi spektroskopisi (FTIR) analizleri kullanılmıştır. SEM sonuçlarına göre, kafeik asitin nanoliflere eklenmesi, daha ince nanolifler elde edilmesine sebep olmuştur. Tüm nanolifler tek tip morfoloji sergilemiştir. Kafeik asit, nanofiberlere verimli bir şekilde yüklenmiştir. Kafeik asit konsantrasyonları %1 den %10 a arttırıldığında, yükleme verimleri %76,4 den %94 e artmıştır. kafeik asit konsantrasyonu %10 olan nanolifler %92,95 antioksidan aktivite göstermiştir. Sonuçlar, elektroeğirme yoluyla kafeik asitin keçiboynuzu unu/peynir altı suyu

proteini konsantresi bazlı nanoliflere kapsüllenmesinin aktif paketleme uygulamaları için uygun bir aday olduğunu göstermiştir.

Anahtar Kelimeler: Aktif paketleme, Biyobozunur paketleme, Elektroeğirme, Keçiboynuzu unu, Kapsülleme

To my beloved family

ACKNOWLEDGMENTS

I would like to express my special thanks and respect to my supervisor Prof. Dr. Serpil Şahin for her continuous support, understanding, guidance, energy and encouragement throughout this study. She has always been tolerant, patient and kind towards me. I am also grateful to my co-advisor Prof. Dr. Gülüm Şumnu for her helpful advice throughout my thesis. I consider myself extremely fortunate to be studying under their wise direction.

Additionally, I also want to express my gratitude to Eda Berk Yıldız, Kübra Ertan, Seren Oğuz, and Selen Güner for helping me with my experiments. Their assistance and kind attitude at work strengthened my motivation.

I would also like to thank my dearest labmate Gizem Aslaner who made me feel very lucky with her friendship and support. My special thanks continue with my oldest friends, Damla Ergeç, Duygu Uylar, and Ertuğrul Çubuk, for their loyalty and for never leaving me alone throughout this time.

Finally, I would like to express my sincere gratitude to my mother, father, sister, brother and nephew for their endless support, unconditional love, patience and being with me in my every decision. They made me feel very fortunate throughout my life. I devoted my work to them.

TABLE OF CONTENTS

LIST OF TABLES

TABLES

LIST OF FIGURES

FIGURES

LIST OF ABBREVIATIONS

ABBREVIATIONS

ΔH_m: Melting enthalpy

AA: Antioxidant activity

CA: Caffeic acid

DSC: Differential scanning calorimeter

FTIR: Fourier-transform infrared spectroscopy

LE: Loading efficiency

PEO: Polyethylene oxide

SEM: Scanning electron microscopy

T_g: Glass transition temperature

T_m: Melting temperature

TGA: Thermogravimetric analysis

XRD: X-ray diffraction

WPC: Whey protein concentrate

WVP: Water vapor permeability

CHAPTER 1

INTRODUCTION

1.1 Encapsulation of Bioactive Ingredients

Environmental factors such as pH, temperature, and light exposure, which can cause antioxidants to deteriorate, limit their bioavailability and bioaccessibility. Encapsulating antioxidants in biopolymer matrices is a successful approach to improve their bioavailability and stability (Celebioglu & Uyar, 2020). A process called encapsulation creates particles with nano, micro, and millimeter-sized diameters by enclosing a component in another material. The active agent, the base material, the fill, the internal phase, or the payload phase are some examples of names for the encapsulated components (Alemzadeh et al., 2020). Using this technique, bioactive substances can be captured and released in a controlled environment. In the food industry, variety of substances, including amino acids, vitamins, minerals, antioxidants, colorants, enzymes, and sweeteners, can be encapsulated. In addition, by shielding bioactive compounds from the damaging effects of oxygen or moisture, encapsulation may encourage higher product stability (Singthong et al., 2014). The entire food cycle process, from manufacturing to storage, has transformed as a result of encapsulation technology. Additionally, it has altered how innovative things are developed and how they are used (Alemzadeh et al., 2020). To encapsulate bioactive substances, a number of approaches have been devised, each having advantages and disadvantages of their own. These methods comprise emulsification, inclusion complexation, nano-precipitation, liposome, spray drying, freeze drying, and others. Due to their straight forward procedures and

accessibility to commercial scale-up, solvent evaporation and spray-drying are the two encapsulating techniques that are utilized the most frequently. However, using a relatively high working temperature when drying could result in thermal damage, which would impact the stability and the effectiveness of encapsulating labile components. For instance, spray drying encapsulation dramatically decreased bacterial viability or harmed the structure of target compounds (Wen et al., 2017). One of the most advantageous methods for materials that are thermosensitive is freeze drying. However, freeze drying is an expensive technique when compared to other techniques (Alemzadeh et al., 2020).

1.2 Electrospinning

Electrospinning has recently been proved to be a very viable method for encapsulating bioactive substances (Celebioglu & Uyar, 2020; Vilchez et al., 2020). It can be used in more advanced scientific and technological fields. Although William Gilbert, an English physicist, first proposed the idea of electrospinning in the 15th century, no researchers have focused on the manufacture of nanofibers since the beginning of this era. Electrostatic spinning is where the word "electrospinning" comes from. William Gilbert created an experimental setting in which he saw that water droplets are initially spherical at the dry surface of the substrate. This observation led Gilbert to theorize that electrostatic attraction between liquids occurs. But when electrostatic force was applied to them, they changed into a cone shape (Amna et al., 2020). The basic idea of electrospraying for electrically distributing fluids, which Cooley (Cooley, 1902) and Morton (Morton, 1902) patented in 1902, was the same as that of electrospinning, which Formhals (Formhals, 1934) patented in 1934. The main distinction between electrospinning and electrospraying is that the latter employed a polymer solution while the former used a low molecular weight solution. Later, Taylor used a mathematical simulation of the electrospinning process to explain how the electric force affected the fluid droplet's ability to form a cone shape, which is known as the Taylor cone. However,

this simulation did not receive much attention until Baumgarten experimentally produced acrylic microfibers using electrostatic spinning in 1971. There have been tremendous advancements in knowledge and applications at the nano- and micro-scales as a result of the fast-moving field of electrospun nanofiber research that has undergone various revolutions during the past two decades (Li et al., 2021). Electrospinning allows the production of fibers with ultra-fine structures, high porosity, a high surface-to-volume ratio, and customized morphology which can be employed in a variety of sectors including biological engineering, environmental protection, and within the energy and food packaging industry. It also has several advantages that make it suitable to produce active food packaging. Since it is a non-thermal process, it allows for the encapsulation of thermosensitive compounds. Furthermore, due to the quick solvent evaporation during operation, the amount of organic solvent in the food system is decreased (Zhang et al., 2020). An electrospinning equipment must have three essential components in order to function: a capillary tube with a needle or pipette, a high power voltage source, and a collector or target. Electrical cables link the high power supply, which holds the polymeric solution, to target and the capillary tube. They are held in close proximity to one another. Targets for collecting fibers during the electrospinning process have included aluminum foil or plates, copper plates, human hands, and rotating drums (Schiffman & Schauer, 2008). In general, this technique enables the polymer solution to flow through an electric field produced between the nozzle and receiver which results the formation of nanofibers (Rani et al., 2021). Using a high-voltage electrostatic field, a large variety of biopolymers, alone or mixed with other components, have been prepared. The surface tension of these polymer solutions is overcome, and the steam ejected from a needle is stretched, which is related to the Taylor cone's instability, by the electric field. Concurrently, the jets partially or completely solidify due to solvent evaporation or cooling, and the fabrication of fibers into sheets or other shapes accelerates (Guan et al., 2020).

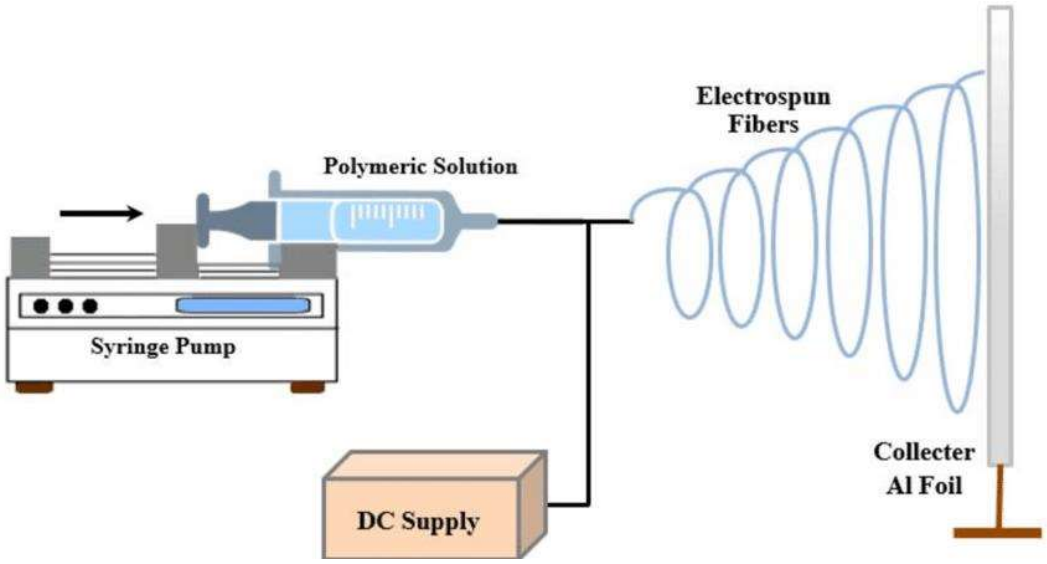

Figure 1.1 Basic representation of electrospinning.

Reprinted from "Highly Hydrophilic Electrospun Polyacrylonitrile/ Polyvinypyrrolidone Nanofibers Incorporated with Gentamicin as Filter Medium for Dam Water and Wastewater Treatment," by R. Asmatulu, 2016, Journal of Membrane and Separation Technology, 5(2), 38–56.

1.2.1 The Parameters Affecting Electrospinning Process

The process of electrospinning is relatively straightforward, but the physics underlying it is complicated since it depends on a number of regulating factors that are peculiar to polymer solutions, including solution viscosity, polymer concentration, solution conductivity, and surface tension. The process parameters—applied voltage, spinneret to collector distance, relative humidity, temperature, and flow rate—are also crucial to pay attention to (Kumar & Sinha-Ray, 2018). A viscoelastic liquid with high electrospinnability can initiate a jet and spin steadily in the presence of an applied electrostatic field, forming continuous fibers with uniform fiber diameter and few bead-on-string defects. In the laboratory, a great deal of research has been done on the materials and processing parameters of electrospinning. Three main factors, including the solution's properties such as viscosity, conductivity, molecular weight, surface tension, and solvent type; the

process parameters which are applied voltage, flow rate, and tip-to-collector distance; and the ambient conditions, humidity, and temperature, tend to influence the process and play a major role (Li et al., 2021).

1.2.1.1 Solution Properties

1.2.1.1.1 Viscosity

One of the most effective factors to affect fiber morphology is viscosity, which measures a material's resistance to flow. The amount of entangled polymer molecule chains in a solution typically correlates with its viscosity (Valizadeh & Farkhani, 2014). The primary force working to counteract Columbic repulsion, which is the primary force driving elongation of the jet after leaving the Taylor cone apex, is the viscoelastic force present within the polymer charged jet (Okutan et al., 2014). Due to the low surface tension, viscous solutions make it difficult for polymers to move through electric jets without generating beads. On the other side, if a solution is less viscous, electrospinning will not ultimately occur (Amna et al., 2020). Typically, the concentration of the polymer in the solution can be changed to tune the viscosity, resulting in the production of various products. A separate polymer or oligomer solution has a different range of viscosity that can be used for electrospinning. It is crucial to understand the relationship between viscosity, polymer concentration, and polymeric molecular weight (Li & Wang, 2013, chap. 2)

1.2.1.1.2 Conductivity

One of the key factors in the electrospinning process is the solution conductivity since more charges may be transported at greater solution conductivities while the viscous polymer solution is being stretched by the repulsion of the charges on its surface (Uyar & Besenbacher, 2008). Compared to synthetic polymers, natural polymers exhibit increased surface tension as a result of their polyelectrolytic nature.

As a result, compared to synthetic fibers, it produces inferior fiber production (Thenmozhi et al., 2017). Salts, ions, or conducting polymers can be added to the polymer solution to boost conductivity, which results in the creation of high-quality nanofibers with fewer flaws and smaller diameters (Aman Mohammadi et al., 2020). Solvents with higher conductivities are frequently used to create polymer solutions in order to boost conductivity. Since the polymer solution is stretched further under the strong electrical field, an increase in the solution's conductivity causes the development of bead-free, uniform, and thinner fibers (Uyar & Besenbacher, 2008).

1.2.1.1.3 Molecular Weight of Polymers and Their Concentration

The concentration of the polymer solution and the polymer molecular weight are two factors that greatly affect the viscosimetric characteristics of the solution and, as a result, can have an impact on the morphology of the fibers (Mercante et al., 2017). The degree of polymer chain entanglement in a solution, or its viscosity, is reflected in the molecular weight (Li & Wang, 2013, chap. 2). High molecular weight polymers have a higher surface area, which makes it easier for polymer chains to entangle, increasing the viscosity of the solution. Larger diameter fiber synthesis has been linked to this rise in viscosity. Similar to this, the number of polymer chains increases with increasing solution concentration. Low concentration solutions have been shown to produce polymer nanofibers with more flaws, such as beads. Extremely concentrated solutions, however, have the potential to produce fibers that resemble ribbons or possibly to impede the electrospinning process (Mercante et al., 2017). Also, electric charges must be transferred from the electrode to the spinning droplet in the electrospinning process. Therefore, a minimum electrical conductivity is necessary for the creation of nanofibers. Nanofibers cannot be electrospun from non-conductive solutions. Type of polymer and solvent, concentration of polymer, and temperature all affect electrical conductivity. The concentration affects the solution conductivity where the polymer possesses ionic capabilities. (Okutan et al., 2014). It is crucial to discover the optimal concentration,

which will rely on the other experimental parameters and the polymer utilized, in order to generate continuous fibers free of flaws (Mercante et al., 2017).

1.2.1.1.4 Surface Tension

The force applied in the surface's plane per unit length is referred to as surface tension. In order to create nanofibers during the electrospin process, the applied voltage must be high enough to overcome the surface tension of the spinning fluid. Surface tension fluctuates to some extent due to solvents (Thenmozhi et al., 2017). Surfactants are frequently used to increase the electrospinnability while also reducing the diameter of the electrospun fibers and promoting uniformity (Castro Coelho et al., 2021). Low surface tension feed solutions result in fibers without beads. Not all solutions with low surface tension, though, can be electrospun. Although not necessarily linearly, the minimum voltage required to produce nanofibers rises as the surface tension of the solution does. Temperature, chemical composition, and concentration all affect how tight a polymer solution's surface tension is (Okutan et al., 2014).

1.2.1.2 Process Parameters

1.2.1.2.1 Flow Rate

Flow rate is another crucial factor for producing successful, attractive electrospun fibers. The flow rate is the quantity of polymer solution that passes through the Taylor cone and needle each second (Aman Mohammadi et al., 2020). It controls fiber diameter and its distribution, initiating droplet shape, the trajectory of jet, maintenance of Taylor cone and deposition area. At high flow rates, larger droplets are formed, which increase the average fiber diameters and bead size. It is believed that at high flow rates there is a limitation with increasing the fiber diameter because the amount of charge and flow rates has not increased simultaneously (Zargham et

al., 2012). When the flow rate reaches a critical point, the jet's transfer rate to the capillary tip outpaces the solution's elimination rate due to the electrical force coming from the tip. A persistent but unstable jet is created as a result of this change in the mass-balance, creating nanofibers with beaded structures (Aman Mohammadi et al., 2020). In rare instances, at a high flow rate, ribbon-like flaws and unspun droplets have also been observed in the literature in addition to bead formation. The non-evaporation of the solvent and the low stretching of the solution in the flight between the needle and metallic collector were primarily responsible for the development of beads and ribbon-like structures with an increased flow velocity. The similar result might potentially be explained by the nanofibers growing in diameter as the flow rate rises (Haider et al., 2018). On the other hand, lower flow rates are more desirable as the solvent will have sufficient time for evaporation. However, when the flow rate is high, a larger volume of solution is drawn from the needle tip, which needs a longer time to dry. In this case, the residual solvent might induce the fibers to merge and make webs instead of fibers. Different modes of charged jet-originating from the Taylor cone-are strongly connected to the flow rate. Various degrees of instability lead to different modes of charged jet, and these are achieved by adjusting the flow rate. These modes affect the average droplet size and fiber diameter distribution. In an optimized flow rate, the Taylor cone is kept stable during the process, which results in the smallest average droplet size and narrowest fiber diameter distribution (Zargham et al., 2012).

1.2.1.2.2 Applied Voltage

Because it affects the nanofiber diameter and provides surface charge on the electrospinning jet, the applied voltage is a crucial component of the electrospinning process. In general, as applied voltage is increased, the electrostatic repulsive forces acting on the fluid jet increase, resulting in a decrease in nanofiber diameters (Okutan et al., 2014). Nonuniform fibers with beads may form at low voltages, but at high voltages, the length of the single jet tends to be slightly reduced, the apex angle of

the Taylor cone increases, and thicker and nonuniform fibers are produced. Additionally, higher voltages will draw the solution from the tip of the needle faster and with a greater volume, resulting in a smaller and less stable Taylor cone (Aman Mohammadi et al., 2020). It is generally accepted that when current is introduced into a solution through a metallic needle at a high voltage, a spherical droplet will deform into a Taylor cone and begin to generate ultrafine nanofibers. Each polymer has a different critical value of applied voltage. The stretching of the polymer solution in conjunction with the charge repulsion within the polymer jet is thought to be the cause of the production of smaller diameter nanofibers with an increase in the applied voltage (Haider et al., 2018). According to Deitzel et al. (2001), change in electrospun fiber morphology for the PEO/water system could be explained by the slope change of the electrospinning current as a function of voltage. If the initial voltage was chosen as 9 kV instead of 5.5 kV, the morphology of the electrospun PEO nanofibers shifts from defect free fibers to fiber mats with a high density of beads. If the slope of the electrospinning current versus voltage plot changes, which occurs at a voltage of about 7 kV, this bead structure starts to predominate. This coincidence suggests that one might be able to regulate the density of bead defects in the electrospun fibers by paying attention on the spinning current.

1.2.1.2.3 Distance between Tip and Collector

The form of an electrospun nanofiber is largely dependent on the distance between the metallic needle tip and collector. Because it depends on the deposition duration, evaporation rate, and whipping or instability interval, the nanofiber form might be easily influenced by the distance (Haider et al., 2018). The fiber will not have enough time to solidify before it reaches the collector if the distance is too close, whereas bead fiber can be produced if the distance is too far. It is well knowledge that the dryness of the electrospun fiber from the solvent is a crucial physical feature; hence, a suitable distance is advised (Li & Wang, 2013, chap. 2). In order to prepare smooth and uniform electrospun nanofibers, a critical distance must be maintained, and any

modifications on either side of the critical distance will modify the morphology of the nanofibers. Many studies have investigated the impact of the distance between the needle tip and collector and come to the conclusion that when this distance is kept small, faulty and big diameter nanofibers are produced, whereas the diameter of the nanofiber dropped as the distance was extended. A modification in the distance between the metallic needle and collector has occasionally been seen to have no impact on the nanofiber's shape (Haider et al., 2018).

1.2.1.3 Ambient Conditions

Humidity and temperature are two connected environmental variables that play a role in the fiber formation technology. Solvent evaporation rate increases as the temperature rises and the humidity decreases. High humidity causes thick fibers with a larger diameter. Increased humidity results in the formation of porous nanofibers. As a result, for appropriate porous nanofibers, an optimal level of humidity should be preserved (Thenmozhi et al., 2017). The temperature of the environment can have a significant impact on both the volatilization of the solvent and the viscosity of the polymer solution. Increasing the temperature reduces the viscosity of the polymer solution and increases the rate of solvent evaporation from the jet surface, resulting in smaller diameter fibers (Aman Mohammadi et al., 2020). The impact of RH on the electrospun fibers ‘morphology is determined by the composition of polymer. In the case of an electrospinning of hydrophobic polymer, water would be nonsolvent resulting in the formation of a dry polymer film around the liquid jet at high RH values. As a result, pores form to allow trapped solvent molecules to evaporate and complete nanofiber solidification. Lower RH values result in faster evaporation of the solvent, resulting in thicker nanofibers. Furthermore, the combination of solution jet solidification rate and capillary break up of viscoelastic fluid was proposed as a mechanism for morphological changes in the electrospun product caused by RH variations during electrospinning. (Pelipenko et al., 2013).

1.2.2 Microwave Heating in Electrospinning

In this study, microwave treatment was selected as heat treatment to increase spinnability of biopolymers. Also, microwave heating was shown to be a good method to provide bead-free homogeneous nanofibers because internal heating generates higher internal pressure which promotes the release of free amino groups and increase in viscosity (Aslaner et al., 2021). Studies related to the microwave pretreated active electrospun nanofibers were very limited. Aslaner et al. (2021) investigated the effect of microwave pretreatment prior to the electrospinning. Conventionally heated solutions and microwave-heated solutions were compared. According to the results of this study, microwave treated samples showed bead-free homogenous nanofibers, lower electrical conductivity, and higher fiber diameter and solution viscosity. Also, it was mentioned that as a result of the potential release of phenolics bound to cell walls during food processing, microwave treatment may have a growing impact on total phenolic content. Additionally, in the study of Uygun et al. (2020), in terms of free amino groups, there was no significant difference between the conventionally heated solution and the unheated solution. In contrast, samples heated conventionally had the lowest amount of free amino group, while samples heated in the microwave had the maximum quantity. Microwave heating promotes protein unfolding and causes an increase in the internal pressure gradient, which can lead to increased release of free amino groups. Microwave treated samples had higher fiber diameter and higher viscosity explained by the increase in free amino groups. The results of both two studies supported that microwave heating increased electrospinnability as bead free homogeneous fibers were obtained as compared to the conventionally heated samples. Also, adding polyethylene oxide (PEO), water soluble, biodegradable thermoplastic polymer, to the whey protein isolate solution were shown to increase the solution's spinnability due to PEO chain entanglement with biopolymer molecules and also the charge-counter-acting effect of PEO on biopolymers (Colín-Orozco et al., 2015; Vega-Lugo & Lim, 2012). Thus, PEO was

added into carob flour-WPC blend in this study to obtain bead free and homogenous nanofibers.

1.3 Active Packaging

Traditional food packaging provides mechanical support as well as protection against environmental hazards such as microorganisms, moisture, oxygen, odors and dust (Zhang et al., 2020). As a result, it delays food deterioration and also facilitates transportation and distribution. Because of their good gas and liquid barrier properties, easy formability, availability, and low cost, petroleum-based synthetic films are used for food packaging. However, they are not biodegradable or sustainable, and they are also the source of significant disposal issues (Chen et al., 2019). Additionally, the active plasticizers in these synthetic polymeric films is leaking to the product which causing food quality to deteriorate, which is extremely dangerous for the food product's safety and shelf life. As a result, the packaging industry is moving toward the usage of biopolymers that are safe, secure, and non-toxic (Rangaraj et al., 2021). Biopolymers are a class of materials derived from naturally occurring and renewable resources. They have the potential to reduce our reliance on the extraction and processing of fossil fuels. Biopolymers are usually inexpensive, non-toxic, nutrient-rich, and edible. Biodegradable films can be made from lipids, polysaccharides, and proteins. In addition, flour can be a good alternative as it contains carbohydrates, protein, and fiber together. In literature, there are studies in which different flour types such as rye, rice, pea, lentil, and carob are used to produce nanofibers by electrospinning (Aslaner et al., 2021; Oguz et al., 2018; Tam et al., 2017; Uygun et al., 2020; Woranuch et al., 2017).

Carob has high fiber content (approximately 18%) mostly cellulose and hemicellulose and also contains approximately 3-4% protein (Papaefstathiou et al., 2018; Zhu et al., 2019). Cellulosic nanofibers are preferred due to their superior water vapor barrier properties with high mechanical strength (Muthu et al., 2019). Pérez et al. (2021) prepared biopolymer films include black carob extract by solvent

casting method for cheese preservation. Their findings discovered a significant correlation between the barrier characteristics of films and the activity of antioxidants on cheese samples. In another study, two antioxidant cellulose biofilm based on the addition of carob seed macerates were created using either an 8% aqueous carob seed ethanol macerate solution or an 8% aqueous carob seed acetone macerate solution. In comparison to the control samples (without an active agent), this study demonstrates the favorable effects of carob seed acetone macerate and carob seed ethanol macerate biopackaging on salmon samples held at 4°C. Satisfactory sensory evaluation results were obtained with samples tolerable between the third and the fifth days (Ouahioune et al., 2022).

Proteins are amphiphilic in nature because of their amino acid composition, and they provide many binding sites for bioactive substances, which is primarily governed by electrostatic attraction, hydrophobic interaction, hydrogen bonding, and covalent bonding. Proteins have several benefits over other materials, which has sparked a lot of interest in producing protein-based electrospun fibers (Zhang et al., 2020). Combining polysaccharides and proteins for food packaging can highlight the strengths of these two components while minimizing their limitations. There are studies in the literature that support this (Aman et al., 2019; Aslaner et al., 2021; Kutzli et al., 2019). Whey is a byproduct of the milk processing industry and is used to make cheese and casein. Whey is very useful to the food sector since it has both functional and nutritional benefits due to its solubility, absorption, water holding capacity, viscosity, emulsifying, foaming, or gelation (Zhong et al., 2018). There are promising studies on the use of whey protein in the production of electrospun nanofibers (Aslaner et al., 2021; Colín-Orozco et al., 2015; Drosou et al., 2018; Kutzli et al., 2019; Sullivan et al., 2014; Vega-Lugo & Lim, 2012; Zhong et al., 2018).

Packaging technologies have advanced significantly in recent years, including active and intelligent packages that promote quality, safety, and product shelf life (Aman Mohammadi et al., 2020). An edible polymer with antioxidants is used in the design of the edible active packaging. The mechanical properties and water vapor/oxygen

resistance of the packaging films are improved by adding natural active agents and nanofillers to the biopolymer solution. Additionally, this strengthens the food product's resistance to oxidation and prevents the formation of bacteria that are associated with food poisoning (Rangaraj et al., 2021). Active food packaging is designed to scavenge undesirable substances or to release preserving agents such as antioxidants or antimicrobial agents (Zhang et al., 2020). In detail, this concept can increase the shelf life of the product by releasing active agents through a controlled mechanism of diffusion from the packaging material to the product and then dissolution in the surface of the product or in the packaging atmosphere, or by scavenging free radicals. On the other hand, non-migratory active packaging works without the migration of the active materials into the products, mostly based on iron oxidation, ascorbic acid oxidation, catechol oxidation or enzymatic catalysis (Sanches-Silva et al., 2014). The active substances (antimicrobial, gas scavenger, antioxidant) that are added to the packaging material or coated onto the surface of it with the intention of extending the shelf life of food and enhancing consumer safety determine the architectures of active food packaging (Gaikwad et al., 2019). Because of their higher ability to exchange hydrogen and single electrons, and the resonance stabilization of the resulting phenolic radicals, phenolic acids can absorb free radicals and thus inhibit food oxidation (Benbettaïeb et al., 2018). Antimicrobial agents can be introduced into the biopolymer matrix to protect food against microbial deterioration and extend shelf life, which has a positive influence on the profit and controlling of the foodborne diseases. Spices, herbs, and their essential oils, chitosan, bacteriocins, ethylenediamine tetraacetic acid, smoke antimicrobials, metal oxides in the form of nanoparticles are some of the active substances that have recently drawn attention (Arkoun et al., 2018). A wide range of antioxidants from synthetic to natural antioxidants has been investigated in order to produce active packaging and coatings. Quality and the shelf life of the food are improved by the migration of the active ingredients from packaging film to food or absorption of the oxidative radicals from the food. The antioxidants operate as a strong barrier against external microbial infections gaining access to the food surface, as well as destroying any oxidative

stress areas that may exist in the food (Rangaraj et al., 2021). According to Shao et al., (2018), pullulan-carboxymethylcellulose sodium nanofibers containing tea polyphenols were shown to reduce weight loss, preserve firmness, and improve strawberry quality during storage significantly. Curcumin-loaded electrospun nanofibers with very high encapsulation efficiency from zein and gelatin could be used as coatings for fatty food products, according to the findings of another study (Alehosseini et al., 2019). Additionally, grape seed extract-incorporated rye flour-WPC fibers and gallic acid-incorporated lentil flour fibers were promising examples of active electrospun nanofibers (Aslaner et al., 2021; Aydogdu, Yildiz, et al., 2019). Insaward et al. (2015) investigated the effect or phenolic acid (caffeic acid, ferulic acid, gallic acid) addition to the characteristics of soy protein films by casting method. According to results of this study, tensile strength increased with increased phenolic concentration. Also, Wrona et al. (2017) studied the green tea, which includes the strong phenolic substances like catechins encapsuleted polyethylene films obtained by casting for preservation of fresh minced meat. Shelf life of fresh minced meat was extended with active films. Caffeic acid (3,4-dihydroxycinnamic acid) is a phenylpropanoid and hydroxycinnamate metabolite found in plant tissues and food sources such as blueberries, apple cider, and coffee drink extracts. It is employed as a carcinogenic inhibitor, which has antioxidant and antibacterial properties in vitro, hence aiding in the prevention of cardiovascular and atherosclerotic illnesses (Luzi et al., 2020). To the best of our knowledge, there is no study in the literature on encapsulation of caffeic acid into biodegradable nanofibers to be used as active packaging material.

1.4 Objective of the Study

The packaging industry has recently paid increasing attention to biodegradable packaging materials because of their sustainability, non-toxicity, and safety. Additionally, biodegradable active packaging increases the food product's resistance to oxidation and extends its shelf life by preventing the growth of pathogens.

Although electrospinning has been used to produce biopolymer nanofibers, there is still a literature gap in active packaging research on the encapsulation of bioactive substances into natural biopolymer matrix. There is literature gap on the applicability of carob flour-based active packaging materials produced by electrospinning and encapsulation of caffeic acid into biodegradable nanofibers as active packaging materials in the literature.

The objective of this study is to encapsulate caffeic acid into biodegradable nanofibers made of carob flour, to be used as active packaging material. Since the protein ratio in carob is low, the addition of WPC was assumed to be more suitable for developing packaging materials in this study. Carob flour/whey protein concentrate blend has never been used as a nanofiber material before. Crystalline structure of the cellulose and the complex secondary and tertiary structures of the proteins make them impractical to produce electrospun nanofibers due to insufficient entanglement. Several methods, such as denaturation, the use of an appropriate solvent, and blending with other polymers, can be used to ensure the successful electrospinning of globular proteins (Muthu et al., 2019; Zhang et al., 2020). Microwave pretreatment was chosen to increase electrospinnability and obtain bead free homogeneous fibers.

CHAPTER 2

MATERIALS AND METHODS

2.1 Materials

Carob flour was purchased from Havancızade Gıda Gıda Co., Inc. (İstanbul, Turkey). Whey protein concentrate (80% protein on a dry-weight basis) was provided from Proteinocean Gıda Co. Inc. (Ankara, Turkey). Caffeic acid (CAS #: 331-39-5), polyethylene oxide (900 kDa molecular weight, CAS #: 25322-68-3), and sodium hydroxide pellets (CAS number: 1310-73-2) were obtained from Sigma Aldrich Chemical Co., (St. Louis, MO, USA). Polyoxyethylene sorbitan monooleate (Tween80) (density: 1.064 g/m3, viscosity: 400–620 cps at 25 °C, CAS #: 9005-65-6) was supplied from Merck (Darmstadt, Germany).

2.2 Solution Preparation

PEO was dissolved in the distilled water with magnetic stirrer (MaxTir 500, DaihanScientific Co, KR) for 24 h at 400 rpm to obtain 2.5% (w/v) homogenized solution. Then, carob flour (3% w/v) and whey protein concentrate (1%, and 3% w/v) were added to the solution at different concentrations (Table 2.1). Solutions were mixed with high-speed homogenizer (IKA T25 Digital Ultra-Turrax; IKA®-Werke GmbH&Co. KG, Staufen, Germany) at 10000 rpm for 3.5 min. pH of the solutions was adjusted to 10 by adding 8 M NaOH. pH of the solutions was measured by pH Portable Meter (SG2 SevenGoTM, Mettler, Toledo, USA). Temperature of the solutions was brought to 80°C by microwave heating (450 W for 2.5 min) (Advantium Oven TM, General Electric Company, Louisville, ABD). At the same time, caffeic acid (CA) was dissolved in 80% aqueous ethanol by magnetic stirrer at 750 rpm for an hour. Then, it was incorporated into the electrospinning solutions to

obtain 1% and 10% (w/w, % in solid fibers) of CA content in solid fibers. Tween80 (2% w/v) was added to the mixtures as surfactant. Then, final solution was stirred further by using magnetic stirrer for 30 min at 750 rpm for complete homogenization.

Table 2.1 Solutions' nomenclature and their composition

Name	Composition
3C1W	3%(w/v) Carob flour-1%(w/v) WPC
3C3W	3%(w/v) Carob flour-3%(w/v) WPC
3C3W1CA	3%(w/v) Carob flour-3%(w/v) WPC-1%(w/w) CA
3C3W10CA	3%(w/v) Carob flour-3%(w/v) WPC- 10%(w/w) CA

2.3 Solution Properties

2.3.1 Rheological Properties

Rheological properties of the solutions were analyzed by a controlled strain rheometer (Kinexus, Pro+ Rheometer, Malvern, UK) with a titanium cone and plate geometry (4° cone, 40 mm diameter, and 1 μm gap) at 25 °C for shear rates varying between 0.1 s^{-1} and 100 s^{-1}. Shear rate versus shear stress values were recorded. Power law model was chosen to determine the flow behavior index (n) and the consistency index (k). Measurements were duplicated.

2.3.2 Electrical Conductivity

Electrical conductivity of the solutions was measured by using conductivity meter (InoLab® Cond 7110, Wissenschaftlich-Technische Werkstätten GmbH, Wheilheim, Germany) at room temperature. Measurements were conducted twice.

2.4 Electrospinning Process

To obtain films made of nanofibers, the electrospinning process was applied. Each solution was put into 5 mL syringe with an inner diameter of 11.53 mm and a 21-gauge steel needle. It was placed horizontally into the electrospinning equipment, which includes a high-voltage source, a syringe pump, and a rectangular metal collector (Nanoweb 103, Mersin, Turkey). The positively charged electrode was linked to the needle while the negatively charged electrode was linked to a metal collector wrapped with aluminum foil. The distance between the collector and the needle's tip was fixed at 0.3 m. Experiments were carried out at room temperature with a relative humidity of 30–40%, a flow rate of 0.8 mL/h, and a voltage of 12 kV.

2.5 Characterization of Films

2.5.1 Morphological Analysis

Samples' morphology was analyzed by using scanning electron microscopy (SEM) (Nova NanoSEM 430, Hillsboro, OR, USA). Samples were coated with gold palladium and scanned at 10,000× magnification level. Diameters of nanofibers were measured from the SEM images by using Image J analysis software V 1.50i (Bethesda, MD, USA). Then, average fiber diameter was calculated from one hundred randomly selected nanofibers for each sample.

2.5.2 Differential Scanning Calorimetry (DSC) analysis

The thermal analysis of the electrospun nanofibers was performed using a differential scanning calorimeter (Pyris 6 DSC, PerkinElmer, Waltham, MA, USA). Approximately 5 mg of sample was put into a hermetically sealed aluminum pan. As a reference, an empty pan was used. After cooling to –60 °C, each pan was heated to 250 °C at a rate of 10 °C/min. The glass transition temperature, melting temperature,

and melting enthalpy of each sample were determined using differential scanning calorimetry thermograms. The DSC measurements were carried out in duplicates (Uygun et al., 2020).

2.5.3 Thermogravimetric Analysis

Thermogravimetric analysis (TGA) was conducted to examine the weight change of the fibers, caffeic acid, whey protein, carob flour, and PEO as a function of temperature by thermo-gravimetric analyzer (Perkin Elmer Pyris 1). About 5 mg of sample in powder form was heated from room temperature to 500 °C at a rate of 10 °C/min with nitrogen (Kuntzler et al., 2018).

2.5.4 X-ray Diffraction

The X-ray diffractometry (XRD) data of the nanofibers were obtained using Ultima IV X-ray diffractometer (Rikagu, Japan) with Cu Kα radiation in a range of 2θ = 5–70° (Neo et al., 2013).

2.5.5 Fourier Transform Infrared Analysis

Nanofibers were analyzed using a Fourier transform infrared (FTIR) spectrometer (IR-Affinity1, Shimadzu Corporation, Kyoto, Japan) with an attenuated total reflectance (ATR) attachment. Data were collected at a resolution of 2 cm^{-1} in the wavenumber range of 4000–600 cm^{-1} (Tatlisu et al., 2019).

2.5.6 Water Vapor Permeability

Modified version of ASTM E-96 method was used to determine water vapor permeability (WVP) (Aslaner et al., 2021). Thickness of each film was measured before the experiment by using digital micrometer (LYK 5202, Loyka, Ankara,

Turkey). Cylindrical test cups with a 0.04 m diameter were filled with 30 mL of distilled water. Films were placed in between the cup and the ring cover of each cup coated with sealant and held with screws around the cup. Then, cups were placed into the desiccator filled by silica gels. Films were assumed to be subjected to 100% RH from the inside. Test cup was weighted initially, and then weight changes of the cups were recorded over 12 h period at 1 h intervals. Measurements were replicated twice. During the measurement, relative humidity (RH) and temperature inside the desiccator were recorded using a digital hydrometer (ThermoPro TP50, Atlanta, GA, USA). From the weight loss versus time graph, water vapor transmission rate (WVTR) was calculated, and WVP was found using the equation below;

$$WVP = \frac{(WVTR \times \Delta X)}{(P_{wi} - P_{wo})} \quad (1)$$

where, WVP: water vapor permeability (g m^{-1} s^{-1} Pa^{-1}),

ΔX: film thickness (m),

WVTR: water vapor transmission rate (g m^{-2} s^{-1}),

P_{wi}: partial pressure of the water vapor inside the cup (Pa),

P_{wo}: partial pressure of the water vapor outside the cup (Pa)

2.5.7 Antioxidant Activity

A modified version of the 2,2- diphenyl-1-picrylhydrazyl (DPPH) technique was used to determine the antioxidant activity of nanofibers containing caffeic acid (Yildiz et al., 2021). 10 mg nanofiber sample was combined with 25 mL of 80% (v/v) ethanol-water solution and left to dissolve for 2 hours before centrifuging at 10000 rpm for 3 min. 0.5 mL was added to 3.5 mL of 0.6 mM DPPH solution and incubated for 1 hour in the dark. A spectrophotometer was used to measure the absorbance at 517 nm (UV 2450, Shimadzu, USA). Control was the mixture of 0.5 mL of 80% (v/v) ethanol-water solution and 3.5 mL of 0.6 mM DPPH solution.

Methanol was used as blank. The measurements were taken twice. Using the formula below, the antioxidant activity (AA%) of the fibers was calculated.

$$\mathrm{AA}(\%) = \frac{\mathrm{A_{control}} - \mathrm{A_{sample}}}{\mathrm{A_{control}}} * 100 \quad (2)$$

where, AA: antioxidant activity of fibers,

$A_{control}$: absorbance of the control sample at 517 nm,

A_{sample}: absorbance of the fibers at 517 nm.

2.5.8 Loading Efficiency

The method described in Aydogdu et al. (2019) was used to determine the loading efficiency of caffeic acid in the nanofibers. A spectrophotometer was used to capture the spectrum of caffeic acid dissolved in 80% ethanol-water solution at 300–600 nm, with maximal absorption at 325 nm. By initially dissolving 10 mg of electrospun fibers in 25 ml of 80% ethanol-water solutions, the loading efficiency of caffeic acid in the electrospun fibers was measured. The absorbance values of solutions at wavelengths of 325 nm were determined using a spectrophotometer after appropriate dilutions were done (UV2450, Shamadzu, Columbia, USA). A preset caffeic acid standard calibration curve was used to determine the quantity of caffeic acid amount in the fibers. Using the formula below, caffeic acid's loading efficiency (LE%) was calculated.

$$\mathrm{LE}(\%) = \frac{(\text{Calculated caffeic acid amount})}{\text{Theoritical caffeic acid amount}} * 100 \quad (3)$$

where, LE: loading efficiency of the fibers.

2.5.9 Biodegradability

The biodegradability of films was assessed with some modification as reported by da da Silva Filipini et al. (2020). Weight fluctuations would be inaccurate due to remaining soil on film surfaces; hence it was evaluated qualitatively. Soil was poured into a cylindrical plastic cup with a diameter of 20 cm and a height of 15 cm. Sample in 2 cm × 3 cm size was placed inside a support and buried in the soil to a depth of 10 cm. The plastic cup was kept at room temperature (21±2 ℃) and relative humidity (65± 5%). To keep the compost moist, water was sprayed once a day. Samples were carefully taken out every five days until complete degradation and recorded by a camera.

2.6 Statistical Analysis

Minitab software was used to conduct statistical analysis (Minitab Inc., State College, USA). ANOVA was used to determine whether there were any significant differences between treatments. Tukey's multiple comparison test was used to determine whether there were significant differences in the data ($p \leq 0.05$).

CHAPTER 3

RESULTS AND DISCUSSION

3.1 Physical Properties of Solutions

3.1.1 Solution Properties and Their Relation to Fiber Morphology

The diameter, size, and morphology of the electrospun nanofibers are all controlled by a variety of parameters, including solution properties, process conditions, and ambient parameters. By adjusting these parameters to meet the needs of the application, various polymers can be electrospun into nanofibers with the desired fiber diameter and morphologies (Muthu et al., 2019). The effect of solution properties which are viscosity and electrical conductivity was investigated in this study by maintaining constant ambient conditions and process parameters. The viscosity of a solution is determined by the interactions of its constituent molecules and is dependent on the concentrations and properties of the solutes and reagents utilized, and also on the pH (Liu et al., 2018). Electrical conductivity facilitates the elongation of droplets and the production of a single or many jets (Aman Mohammadi et al., 2020). A solution with low conductivity produces fibers with larger diameters, whereas a solution with high conductivity can produce excessively small fibers like spider-net fibers. As a result of the solution's efficient conductivity, the electrostatic interaction on the jet increases, and simultaneous effective jet elongation results in fibers with the smallest diameter. Thus, conductivity can help to achieve the desired fiber diameter and morphology (Ashraf et al., 2019). In Table 3.1, consistency index (k), flow behavior index (n), the electrical conductivity of the solutions, and the average diameters of electrospun fibers obtained from solutions with different WPC and CA concentrations can be seen.

Table 3.1 Properties of solution and average fiber diameter

Solutions	n	k (Pa s^n)	Electrical Conductivity (mS/cm)	Average Fiber Diameter (nm)
3C1W	$0.9121\pm0.0013^{a*}$	0.386 ± 0.020^{c}	4.03 ± 0.03^{c}	242 ± 56^{bc}
3C3W	0.9124 ± 0.0086^{a}	0.545 ± 0.012^{a}	4.10 ± 0.01^{c}	310 ± 70^{a}
3C3W1CA	0.9215 ± 0.0002^{a}	0.451 ± 0.015^{b}	4.78 ± 0.03^{b}	257 ± 66^{b}
3C3W10CA	0.9330 ± 0.0175^{a}	0.267 ± 0.002^{d}	5.69 ± 0.12^{a}	222 ± 49^{c}

*Columns having different letters are significantly different ($p\leq0.05$).

k= consistency index, n: flow behavior index.

Fig. 3.1 shows the apparent viscosity versus shear rate graph of the solutions. The Power Law model was followed by all electrospinning solutions, which had high coefficients of determination values ($r^2\geq0.997$).

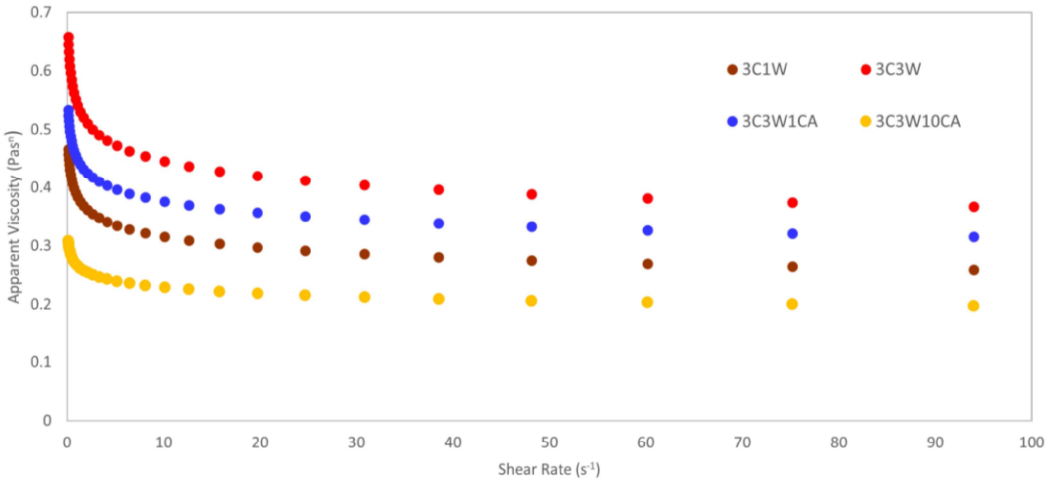

Figure 3.1 Apparent viscosity of the solutions with respect to shear rate

Shear-thinning behavior was observed since the apparent viscosity of the solutions decreased as the shear rate increased. Flow behavior index values (n), which were less than 1, also validated that the solutions had shear-thinning properties. Shear-thinning behavior has also been observed in other electrospinning studies (Aslaner et al., 2021; Aydogdu, Kirtil, et al., 2018; Beikzadeh et al., 2020; Yildiz et al., 2021). The highest consistency index value was found in the solution with the highest whey protein concentration containing no caffeic acid. Also, k value increased from 0.386 to 0.545 when the WPC concentration increased. Similarly, in the previous studies it was found that addition of whey protein increased the viscosity of the electrospinning solution, resulting in the formation of continuous bead-free nanofibers. In these studies, it was discovered that by supporting the whey protein with well spinnable polymers such as PEO and performing other treatments such as changing the pH of the solutions far away from their isoelectric point or applying heat treatment, the protein unfolding and amino group release were accelerated and the molecular entanglement in the polymer solution was increased (Aslaner et al., 2021; Sullivan et al., 2014; Vega-Lugo & Lim, 2012; Wilk & Benko, 2021; Zhong et al., 2018). The same trend was observed in apparent viscosity. By increasing the WPC concentration from 1% to 3%, the apparent viscosities of the solutions increased (Fig. 3.1). The apparent viscosity of polymer solutions is a function of their concentration and molecular weight. This helps us to explain why apparent viscosity increases as protein content increases (Kutzli et al., 2019). Furthermore, there was a significant positive correlation between consistency index and average fiber diameter ($r=0.948$, $p=0.05$). Average fiber diameters of the films were ranged between 222 nm and 310 nm. The sample of 3C3W presented the highest average fiber diameter (310±70 nm). Higher k values in solutions resulted in nanofibers with higher diameters as the number of molecular entanglements in the solution increased (Aydogdu, Sumnu, et al., 2019). In addition, when the amount of caffeic acid in the solution was increased, the k values decreased from 0.451 to 0.267. Caffeic acid was dissolved in ethanol/water solution and then added to Carob/WPC/PEO solutions. As the amount of caffeic acid in the solution increased, the amount of ethanol/water in the solution

also increased. As a result, the solution became less viscous and k value decreased significantly. Similarly, gallic acid-added electrospun nanofibers showed lower apparent viscosity than those without the gallic acid (Aydogdu, Sumnu, et al., 2019). Fig. 3.2 shows the SEM images and the diameter distributions of the nanofibers. According to the SEM images, bead-free, homogenous nanofibers were obtained from the different carob flour-WPC combinations.

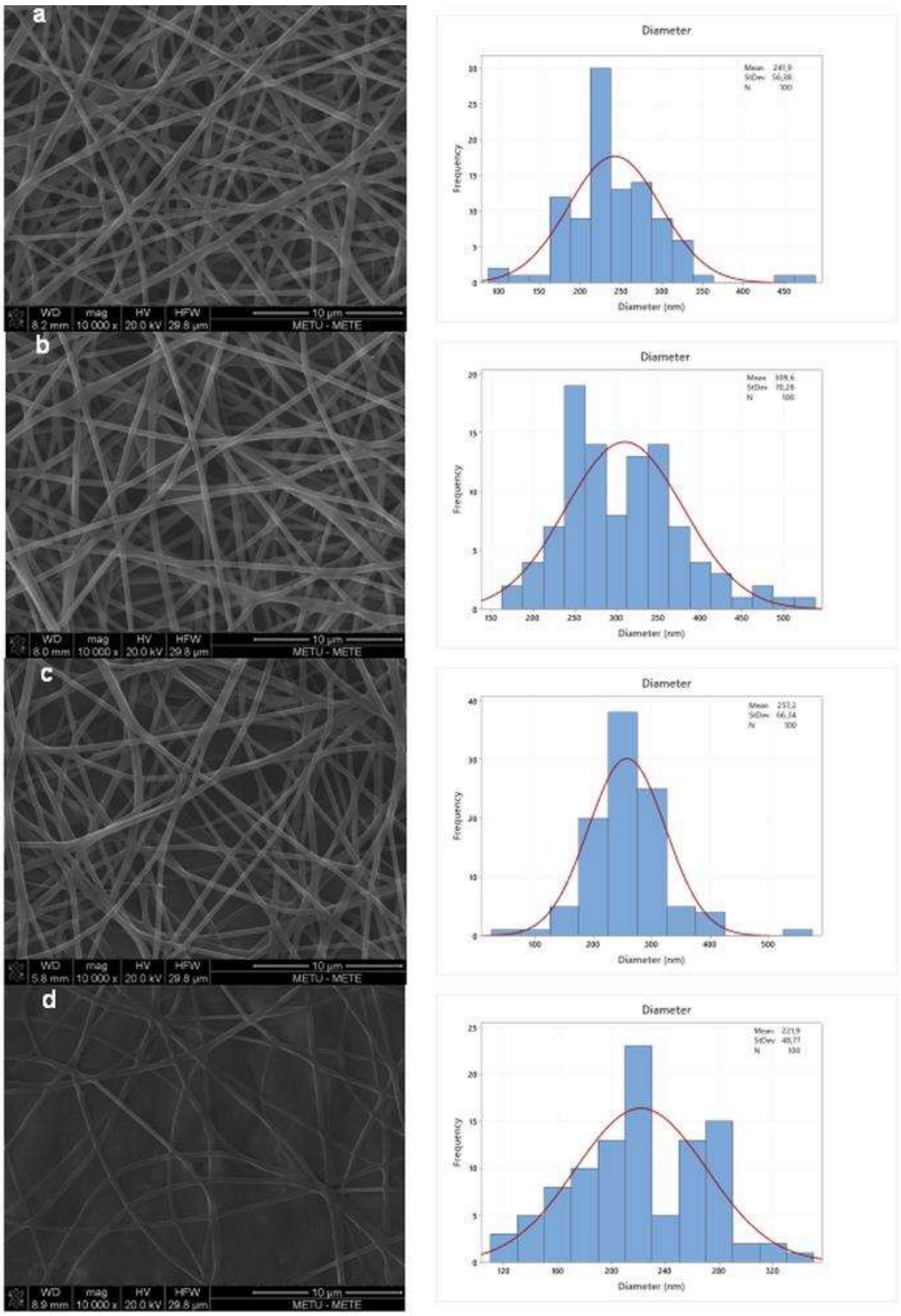

Figure 3.2 SEM images and fiber diameter distributions of the nanofibers: (a) 3C1W, (b) 3C3W, (c) 3C3W1CA, and (d) 3C3W10CA

The addition of WPC reduced the sticky appearance of the nanofibers. In addition, as shown in Fig. 3.2, encapsulating caffeic acid into the nanofibers did not destroy the nanofiber structure and continuous bead-free nanofibers were obtained. As can be seen in Table 3.1, an increase in the whey protein concentration did not affect the electrical conductivity of the solution significantly. However, the addition of caffeic acid and the increase in the caffeic acid content increased the conductivity of solution significantly ($p<0.05$). After the addition of caffeic acid to the solution, the pH of the solution was adjusted again to alkaline conditions with the addition of NaOH. Alkaline solutions contain many Na+ and OH- ions thus causing an increase in the conductivity (Vega-Lugo & Lim, 2012). When conductivity increased, there was a decrease in the average fiber diameter. Similar to the study of (Aydogdu, Sumnu, et al., 2019), the nanofiber sample with the smallest average diameter has been obtained from the solutions having the highest conductivity. As a result, it is reasonable to state that decreasing solution's viscosity while increasing solution conductivity promotes the formation of smooth fibers with smaller diameters, increasing the solution's elongation capacity (Aman et al., 2019). The same trend has been observed in polylactic acid/tea polyphenol nanofibers as the tea polyphenol concentration increased in which fiber diameter decreased from 753 nm to 493 nm. As the tea polyphenol content of the spinning solution increased, so did the solution's conductivity, which resulted in increased electrostatic repulsion between ejection flows and the formation of thinner ejection flows; eventually, smaller diameter fibers were collected (Liu et al., 2018).

3.1.2 Differential Scanning Calorimetry

Table 3.2 shows the glass transition temperature (T_g), the melting temperature (T_m) and enthalpy change (ΔH_m) of the nanofibers.

Table 3.2 Glass transition temperature, melting temperature, and melting enthalpy of nanofibers

Sample	T_g(°C)	T_m(°C)	ΔH_m(J g^{-1})
3C1W	-5.28±0.877[a*]	63.9±0.141[a]	40.89±0.156[a]
3C3W	-9.36±0.509[b]	60.92±0.113[b]	36.47±0.665[b]
3C3W1CA	-9.83±0.467[b]	61.05±0.071[b]	28.15±0.071[c]
3C3W10CA	-9.47±0.240[b]	62.71±0.580[a]	28.16±0.226[c]

*Columns having different letters are significantly different ($p \leq 0.05$).

The glass transition temperature (T_g) is related to the softening point from glassy state to rubbery state. T_g values of nanofibers decreased significantly with increase in WPC concentration. Also, in the study of Ignatova et al. (2016) due to the increase in the hydrogen bond formation between the water molecules and hydroxyl residues on the polymer chains which had a plasticization effect, T_g decreased. Having both T_m and T_g values, indicates that nanofibers had a semi-crystalline structure showing both amorphous and crystalline property. T_m indicates the melting point of the crystalline phase. Melting temperature of the nanofibers varied between 60.9-63.9 °C which was lower than melting temperature of pure PEO. T_m of PEO was reported as 71.5 °C (Uygun et al., 2020). Similar results were also seen in the different studies (Aslaner et al., 2021; Aydogdu, Yildiz, et al., 2019; Kuntzler et al., 2018; Uygun et al., 2020; Yildiz et al., 2021). One of the reasons for the depression in the melting temperature and the enthalpy might be related to the interaction between PEO and other polymers, carob flour and whey protein. This interaction might have disrupted the crystallinity of PEO. Moreover, the decrease in T_m was higher when the whey protein concentration increased, supporting this reason. The other reason might be related to the working principle of electrospinning. During electrospinning, the rapid solidification process of the stretched chains causes the polymer chains to remain in a mostly non-crystalline state (Yildiz et al., 2021). Melting point of the crystal caffeic

acid was recorded as 203°C (Ignatova et al., 2016). No peak corresponding to that temperature was found in the DSC thermograms of the nanofibers containing 1% and 10% caffeic acid, showing that CA was encapsulated in the nanofibers successfully.

3.1.3 Thermogravimetric Analysis

TGA is a method of determining the thermal stability of materials by measuring the weight change as a function of temperature. Fig. 3.3 depicts the weight loss curve of polymers and fibers against temperature.

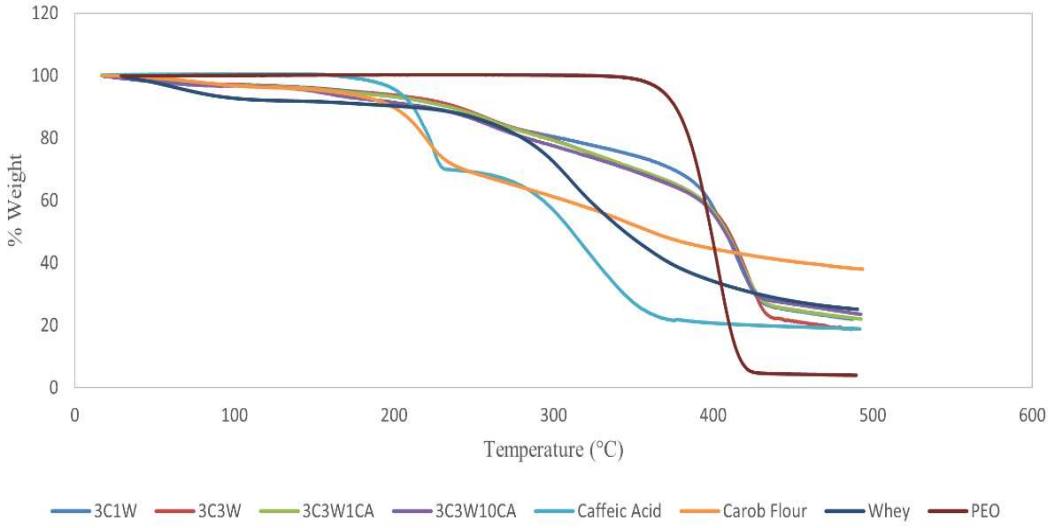

Figure 3.3 Thermogravimetric curves of the electrospun nanofibers, carob flour, WPC, PEO, CA

PEO had one degradation stage with a beginning temperature of roughly 350 °C, and at almost 410°C, nearly 95% of the sample weight degraded. Carob flour showed two stage degradation at around 220 °C, and 350 °C. T_{onset} of whey protein was nearly at 270°C and at the end of the experiment nearly 20% of the sample weight remained. Caffeic acid, which was stable up to 150 °C, showed two thermal degradation steps at nearly 230 °C and 325 °C, respectively. The first stage of weight loss combines melting and degradation of CA while the second decomposition step might be linked to acid decarboxylation (Luzi et al., 2020). The nanofibers had a two-stage

degradation profile, but the TGA of all nanofibers had a slight initial weight loss up to 100 °C due to the evaporation of solvents mostly free water. The first degradation took place between 200 and 300 °C, which might be linked to polysaccharide and whey protein degradation while the second degradation took place between 400 and 450 °C, which could be linked to PEO degradation. The same trend has also been observed in rye flour-based nanofibers (Aslaner et al., 2021). Furthermore, the nanofibers' 80 % weight degradation temperature was 50 °C greater than the temperature of pure powdered PEO. These variations could be explained by the amounts of these compounds in the fibers, as well as their varying abilities to form hydrogen bonds, which could improve heat stability, as found by Colín-Orozco et al. (2015). The first degradation curve of the caffeic acid added nanofibers was similar to that of 3C3W, while the second one had a lower slope. This finding suggested that the caffeic acid addition slowed down the heat degradation, implying a strong influence on intermolecular interactions as well as its ability to scavenge radicals generating during thermal degradation (Yildiz et al., 2021). Furthermore, whereas caffeic acid degraded at 325 °C, active nanofibers showed no additional weight loss at that temperature, indicating the successful encapsulation and thermally stabilized caffeic acid components. Caffeic acid has also been observed to improve thermal properties of nanofibers in other studies. Main degradation temperatures of the ethylene vinyl alcohol copolymer and caffeic acid-based films increased about 25 °C (Luzi et al., 2020). Also, caffeic acid addition to polypropylene films showed improved thermal resistance than flavanones, chlorogenic and trans-ferulic acids. This was explained by the enhanced antioxidant property due to additional resonance with the presence of a second hydroxyl group in the ortho- or para- position. Because of the high density of conjugated structures, they are particularly effective at scavenging free radicals and thereby slowing down the thermo-oxidative degradation process (Hernández-Fernández et al., 2019).

3.1.4 X-ray Diffraction

All four samples had a similar diffraction pattern with two highly reflected peaks, according to the XRD results presented in Fig. 4. Thus, the composite nanofiber samples are semi-crystalline materials with both amorphous and crystalline structures by exhibiting broad peaks of low intensity.

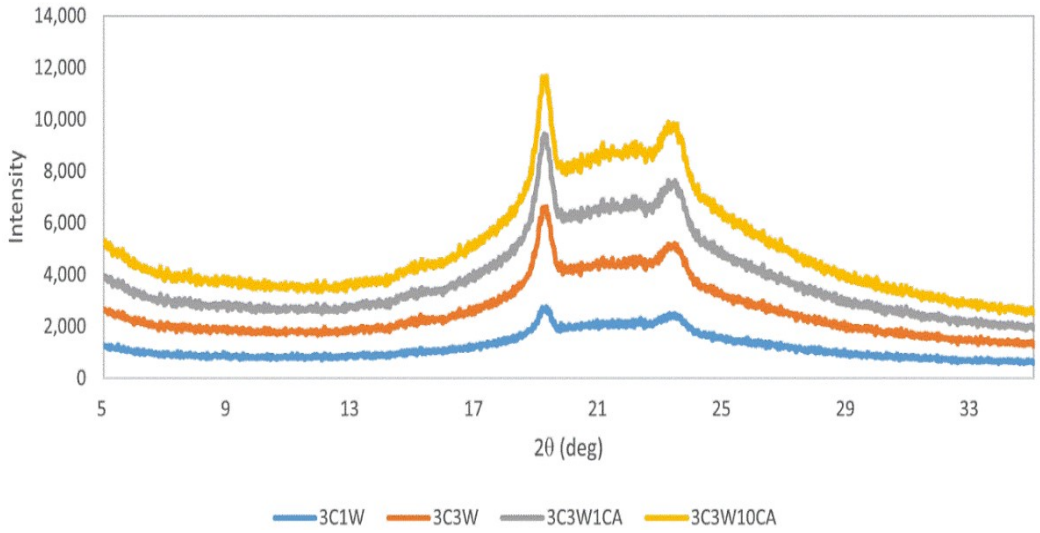

Figure 3.4 X-ray diffractogram of electrospun nanofibers

At 2θ =19° and 2θ=23°, all samples displayed distinct peaks. The crystallinity of PEO could be responsible for those peaks. XRD examination of pure PEO revealed peaks at 19.03° and 23.20° in previous research (Kuntzler et al., 2018). Similar peaks could account for the homogeneous distribution of carob flour, whey protein, and caffeic acid through PEO. They did not appear to have any unusual crystal formations. This also demonstrated how materials interacted powerfully (Uygun et al., 2020). As seen in DSC results (Table 3), XRD results also showed that the interaction of PEO with other polymers in the solution, increasing the whey protein concentration, or the nature of the electrospinning might have resulted in lower crystallinity than PEO. Another reason could be the rapid solvent evaporation during electrospinning as explained in the study of Ignatova et al. (2018). The rapid solvent evaporation may also be responsible for the amorphous state of caffeic acid

phenethyl ester in electrospun fiber mats, resulting in inadequate drying time for the molecular organization required to form a crystal lattice (Ignatova et al., 2018).

3.1.5 Fourier Transform Infrared Analysis

Fourier transform infrared spectroscopy (FTIR) was used to detect the interactions and linkages in the structure of nanofibers. FTIR spectra of the nanofibers is shown in Fig. 3.5.

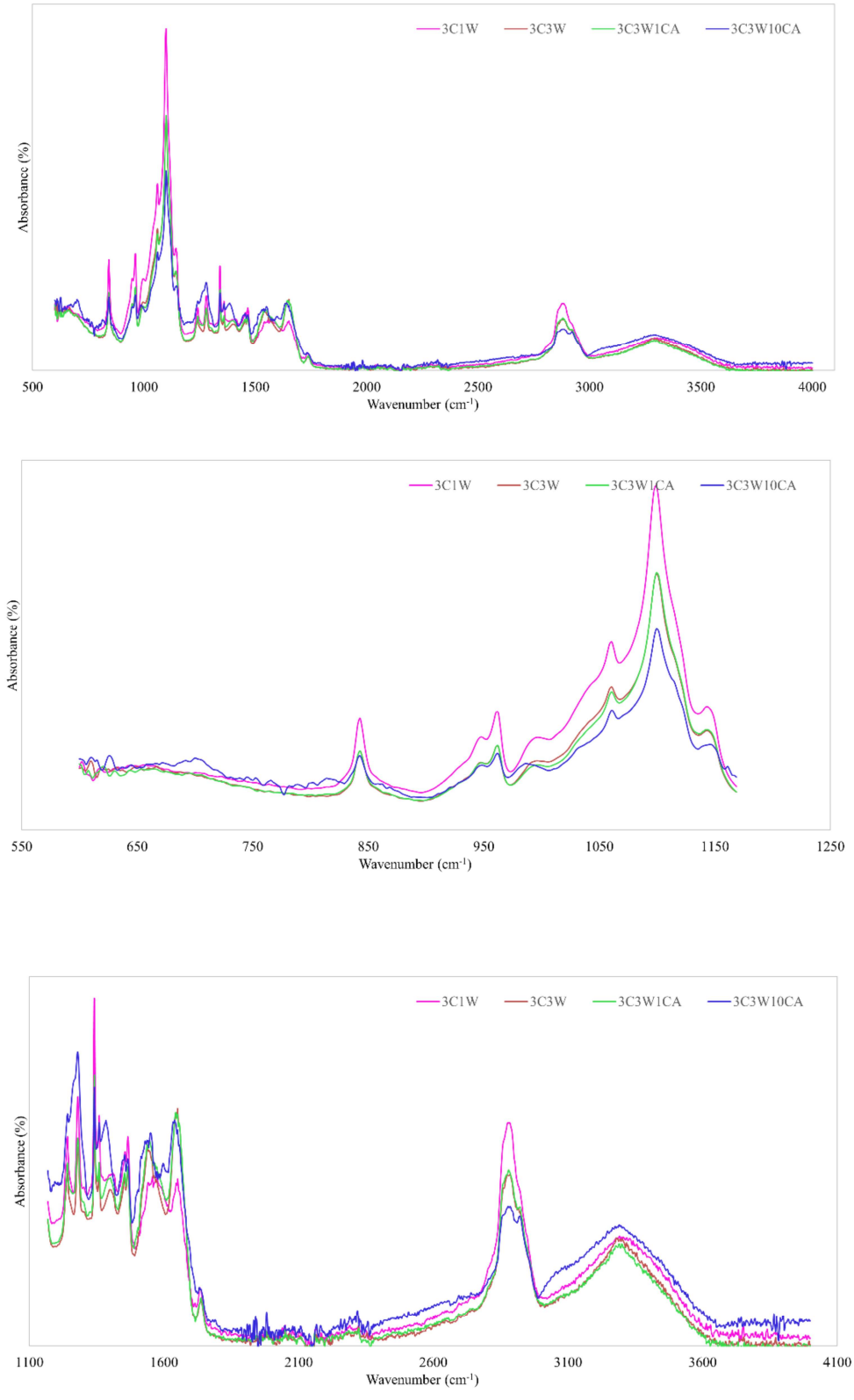

Figure 3.5 FTIR spectra of nanofibers

The presence of the PEO was confirmed by the peaks of about 1100 cm^{-1} and 2850 cm^{-1}. Peaks at roughly 2850 cm^{-1} belongs to the methylene group molecular stretching, whereas peaks at 1100 cm^{-1} corresponds to the combination of the ether and stretching methylene groups in PEO, as indicated in the previous studies (Nikbaht et al., 2020; Sullivan et al., 2014). Peaks in the 1500-1700 cm^{-1} region and also the increase in the peak intensity parallel to the WPC concentration indicated the presence of WPC. The nanofibers' spectra revealed a distinctive peak about 1650 cm^{-1}, which was linked to the Amide-I region and found in proteins. The Amide-II band, which occurs predominantly owing to N=H in-plane bending vibrations, is ascribed to the band that appears at around 1540 cm^{-1}. This peak was also visible in the spectrum of pure whey protein powder (Aslaner et al., 2021; Sullivan et al., 2014). As it was explained in Uygun et al. (2020), which also worked with carob flour, the peaks located around 960 cm^{-1} belonged to the section of starch, amylose, and amylopectin monomer glucose units which was found in the carob flour. Peaks near 960 cm^{-1} in the spectra of nanofibers were attributed to vibrations caused by C-O-C glycosidic linkages. The resulting composite fibers retained all the characteristic bands associated with PEO, carob flour, and WPC. However, minor differences in the spectra of caffeic acid encapsulated nanofiber were discovered. Similar to another study revealed the spectrum of caffeic acid, peaks at 1650 cm^{-1} due to carboxyl group (C=O), 1614 cm^{-1}, 1608 cm^{-1} and 1456 cm^{-1} coming from aromatic ring (C=C) was observed (Yu et al., 2013). The shifting of the bands, such as the amide-III peak shifting from 1298 cm^{-1} (3C3W) to 1276 cm^{-1} (3C3W10CA) and also changing of the peak intensities, for example methylene stretching at 2850 cm^{-1} was less intense for caffeic acid added films than the control film, could be attributed to an interaction between caffeic acid and the polymers in the nanofiber’s composition. The shift in the amide-III was also observed in the caffeic acid containing starch-chitosan film. It was suggested that this might be due to the electrostatic interaction between the charged amino group (NH^{+3}) of chitosan (or gelatin) and the charged carboxylic group (COO^{-}) of antioxidants' phenolic ring (ferulic acid and caffeic acid)

(Benbettaieb et al., 2018). These findings show that caffeic acid was successfully incorporated into electrospun nanofibers.

3.1.6 Water Vapor Permeability

One of the most essential features in food packaging applications is water vapor permeability (WVP). Food packaging materials with adequate barrier qualities can improve packaging conditions by reducing moisture transfer between the food product and the environment (Araghi et al., 2015). The WVP values of the electrospun nanofibers can be seen in Table 3.3, which varied between 1.38-2.95×10^{-10} $gm^{-1}s^{-1}Pa^{-1}$.

Table 3.3 Water vapor permeabilities of nanofibers

Sample	WVPx10^{-10} ($gs^{-1}m^{-1}Pa^{-1}$)
3C1W	$2.95\pm0.21^{a*}$
3C3W	1.38 ± 0.14^{c}
3C3W1CA	2.06 ± 0.08^{b}
3C3W10CA	1.91 ± 0.10^{bc}

*Columns having different letters are significantly different ($p\leq0.05$).

The comparison of WVP values between different samples revealed the effect of whey protein concentration variation in nanofibers and antioxidant incorporation into nanofibers. In another study, WVP of carob/rice starch/PEO blend electrospun fibers ranged between 1.68-2.73x10^{-12} g m^{-1} s^{-1} Pa^{-1} (Uygun et al., 2020). The WVP difference between the studies can be explained by the composition and concentration difference of the solutions, since PEO concentration was higher, and WPC was used instead of rice starch in our study. The hydrophilic nature of both WPC and PEO contributed to the higher water vapor permeability. According to our result, while nanofibers with 3% WPC have the highest barrier property against

water vapor, 1% WPC has the lowest barrier property. The diameter of the nanofibers and the water vapor barrier characteristic have a positive relationship (Aydogdu, Sumnu, et al., 2018). Nanofibers with a high polymer content had a significantly larger diameter and lower WVP values. Similarly, it was observed that WVP values of the nanofibers decreased as the total polymer content of the solutions increased. The increased number of fiber junctions might explain the reason behind that because the porosity of electrospun mat decreased as the fiber diameter increased. The porosity of nanofibers has been shown to have an effect on the WVP values. Also, as the polymer concentration increased, the viscosity increased, reducing the mobility of molecules. Thus, fibers with a high total polymer content exhibited a high viscosity and low water vapor transfer (Aydogdu, Sumnu, et al., 2018). In another study, addition of lime peel extract to the lime peel pectin films lowered the WVP. The film compositions, whether hydrophilic or hydrophobic, and concentration may clarify the distinct behavior of film WVP values due to the molecular interactions between the film matrix and the extract, such as the tortuosity pathway of water molecules (Rodsamran & Sothornvit, 2019). Although change in the caffeic acid concentration did not significantly affect the WVP, addition of the caffeic acid had a significant increase in the WVP. As it was explained in the previous sections, although the hydrophobic property of phenolic acids disrupts water vapor transport through the films, addition of ethanol causes decreases in solution viscosity and fiber diameter. Decrease in the fiber diameter might have an influence on increase in the WVP. An increase in the caffeic acid concentration led to a slight decrease in the WVP. In the study of Araghi et al. (2015), caffeic acid addition to the fish gelatin has a positive effect on permeability. However, the concentration changes of ferulic acid had no effect on the water vapor permeability of fish gelatin. It could be due to the significant amount of hydroxyl groups in ferulic acid that can bind with water. In another study, the addition of unoxidized phenolic acids (ferulic, caffeic, and gallic acid) had no significant effect on the WVP of soy protein film (Insaward et al., 2015).

3.1.7 Loading Efficiency (LE%) and Antioxidant Activity (AA%)

The loading efficiency of the caffeic acid into the nanofibers and the antioxidant activity of the nanofibers were given in Table 3.4.

Table 3.4 Loading efficiency and antioxidant properties of nanofibers containing different amounts of CA and control sample (3C3W)

Sample	LE(%)	AA(%)
3C3W	-	0.85 ± 0.03^{c}
3C3W1CA	$76.4\pm1.3^{b*}$	31.47 ± 0.69^{b}
3C3W10CA	94.0 ± 1.7^{a}	92.95 ± 1.19^{a}

*Columns having different letters are significantly different ($p\leq0.05$).

The loading efficiencies were 76.4% and 94.0% for 1% and 10% CA concentrations respectively. It can be concluded that electrospinning is a very efficient process for encapsulating sensitive bioactive compounds since it is performed at room temperature. Nanofibers containing 10% caffeic acid had extremely high encapsulation efficiency. It was higher than those previously reported for other encapsulation technologies were. In the study of Fathi et al. (2013), the encapsulation efficiency of the caffeic acid-loaded solid lipid nanoparticles was 71.21%. Encapsulation of caffeic acid phenethyl ester in skim milk microcapsules via spray drying reached 41.7% encapsulation efficiency (Wang et al., 2020). Caffeic acid (3,4-dihydroxycinnamic acid) found in various agricultural foods functions as an antioxidant by scavenging oxygen-free radicals and chelating prooxidant metal ions (Fathi et al., 2013). Due to increased resonance stabilization and o-quinone or p-quinone production, the presence of a second hydroxyl group in the ortho- or para-position is known to boost antioxidative activity. This helps to explain why caffeic acid and its phenethyl ester have such great antioxidative activity (Chen & Ho, 1997). 3C3W had 0.85% antioxidant activity, which was coming from the phenolic compounds which was already found in the carob flour. Also, previous studies proved that carob flour has bioactive substances (Youssef et al., 2013; Zhu et al., 2019). As the caffeic acid concentration increased, so did their antioxidant activity, which is also indicated by the effective electrospinning encapsulation.

3.1.8 Biodegradability

Biodegradation is the biochemical material conversion process in water, biomass, carbon dioxide, or methane. The biodegradation of the polymer is divided into two stages. First, the process of reducing polymer chain carbon bond breakage in terms of heat, humidity, and the presence of microorganisms occurs. Second, when shorter chains become energy sources for microorganisms which are bacteria, fungi, or algae, part of the biodegradation process begins. Complete biodegradation is achieved when carbon compounds are converted into water, biomass, or carbon dioxide by micro-organisms (Ivanković et al., 2017). Biodegradation of the films in the soil was observed visually (Figure 3.6).

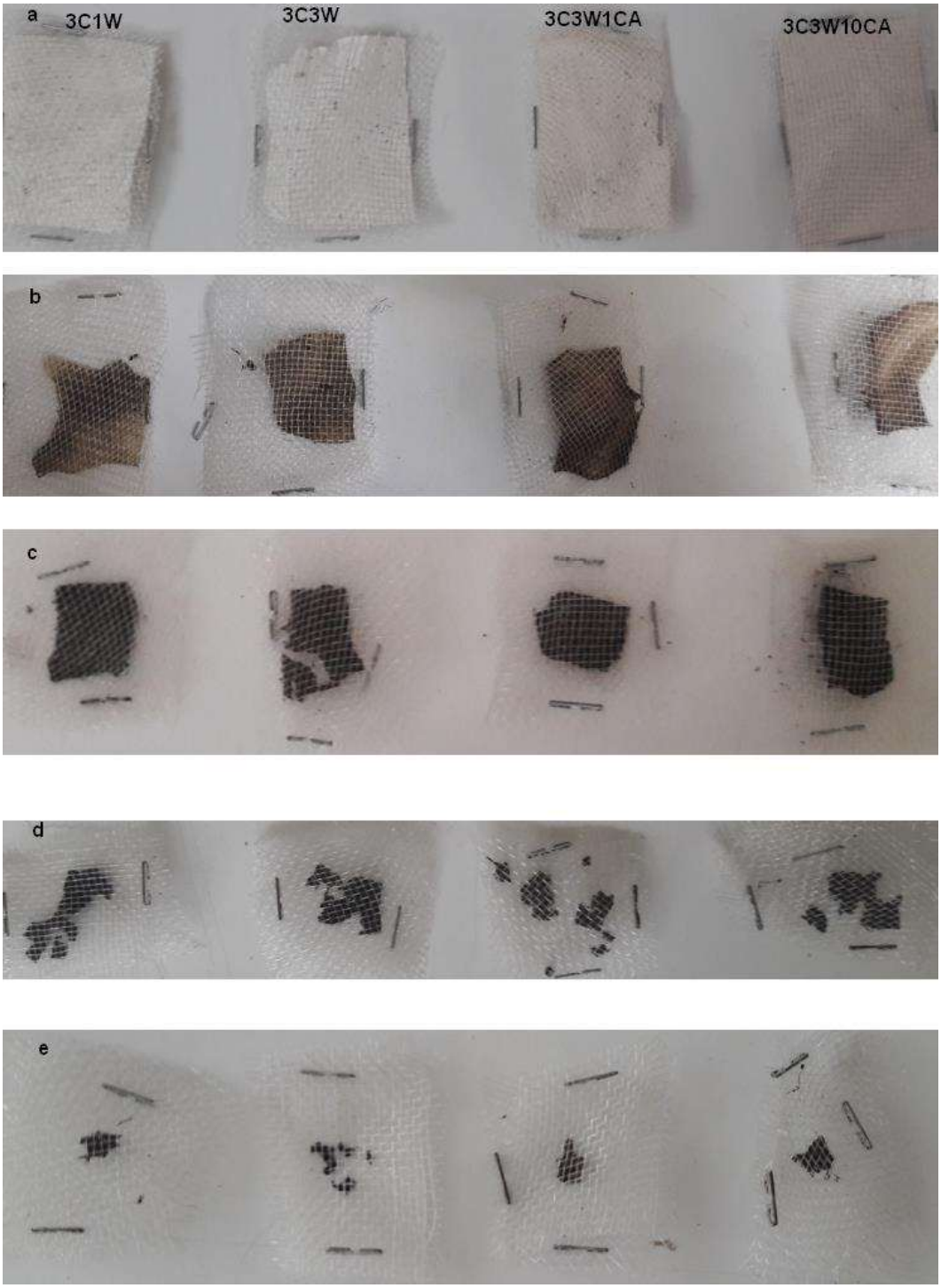

Figure 3.6 Biodegradability of films at the (a) beginning, (b) 5th day, (c) 10th day, (d) 15th day, (e) and 20th day; order of the samples in each row: 3C1W, 3C3W, 3C3W1CA, and 3C3W10CA

The reduction in the area of the biodegraded films was observed every five days until the degradation was complete. The first sign of deterioration in the films was a shift in color. At the end of the fifth day, the color of the films had darkened, and the films had shrunk. In the following days, original appearance and structural integrity of the films had been deteriorated, revealing rougher, degraded surfaces with porous pits and holes. After 15 days, the films were significantly disintegrated. At the end of the 20th day, the areas of the samples were significantly reduced. da Silva Filipini et al. (2020) reported that because of their sensitivity to water, films with high solubility tend to biodegrade quickly because the components of the film structure are available for microorganisms to digest. Additionally, Alqahtani et al. (2021) stated that the weight loss could be a result of the soil microflora disintegrating or the film components becoming soluble due to the addition of water to the soil. In the literature, cassava starch films with natural extracts (green tea and basil) (Medina-Jaramillo et al., 2017) and with yerba mate extract (Medina Jaramillo et al., 2016) showed a degradation time of 12 days, and methylcellulose and jambolao (Syzygium cumini) skins extract films showed a degradation time of 15 days (Medina Jaramillo et al., 2016). All the films produced in the present study are biodegradable. This is a promising result for environmentally friendly applications.

CHAPTER 4

CONCLUSION AND RECOMMENDATIONS

Caffeic acid was successfully encapsulated in carob flour and whey-protein-based electrospun nanofibers in this study. The increase in the WPC concentration led to an increase in the fiber diameter; thus, water vapor barrier properties were improved from 2.95×10^{-10} to 1.38×10^{-10} $g \cdot s^{-1} \cdot m^{-1} \cdot Pa^{-1}$. Also, diameter of the nanofibers were increased with the increase in electrical conductivity of the solution due to increase in the number of molecular entanglements in the solution. CA inclusion in carob–WPC–PEO electrospun nanofibers was validated morphologically, chemically, and thermally. When the concentration of CA was increased, the diameter of the fibers decreased. CA nanofibers synthesized in this study exhibited a uniform and bead-free structure. The FTIR spectrum confirmed that there was a molecular interaction between CA and carob–WPC–PEO. Nanofibers containing 10% CA with 94% loading efficiency have shown that electrospinning is an effective approach for encapsulating bioactive materials into biomaterials. These nanofibers had very high antioxidant activity (92.95%), proving that CA is a suitable material for active packaging because of its antioxidant characteristics. TGA and DSC results supported the loading efficiency findings. According to the TGA results, active nanofibers showed no additional weight loss at 325 °C (one of the degradation temperatures of caffeic acid) indicating the successful encapsulation and thermally stabilized caffeic acid components. According to the biodegradability results, at the end of the 20^{th} day, significant reduction in nanofibers was observed. Finally, CA-loaded environmentally friendly nanofibers developed in this study may be a promising material for novel active packaging applications requiring a high antioxidant activity and biodegradation rate. Due to their weak mechanical capabilities, it is advised to make combinations between these nanofiber films and

another packaging films to obtain multilayered packaging for stronger mechanical properties.

For future studies, the release kinetics of antioxidants and their effects on the shelf life of the products could be investigated in order to assess their potential use in the packaging industry.

REFERENCES

Alehosseini, A., Gómez-mascaraque, L. G., Ghorani, B., & López-rubio, A. (2019). LWT - Food Science and Technology Stabilization of a saffron extract through its encapsulation within electrospun / electrosprayed zein structures. *LWT - Food Science and Technology*, *113*(March), 108280. https://doi.org/10.1016/j.lwt.2019.108280

Alemzadeh, I., Hajiabbas, M., Pakzad, H., Sajadi Dehkordi, S., & Vossoughi, A. (2020). Encapsulation of food components and bioactive ingredients and targeted release. *International Journal of Engineering, Transactions A: Basics*, *33*(1), 1–11. https://doi.org/10.5829/ije.2020.33.01a.01

Alqahtani, N., Alnemr, T., & Ali, S. (2021). Development of low-cost biodegradable films from corn starch and date palm pits (Phoenix dactylifera). *Food Bioscience*, *42*. https://doi.org/10.1016/j.fbio.2021.101199

Aman, M., Ramazani, S., Rostami, M., Raeisi, M., Tabibiazar, M., & Ghorbani, M. (2019). Food Hydrocolloids Fabrication of food-grade nano fi bers of whey protein Isolate – Guar gum using the electrospinning method. *Food Hydrocolloids*, *90*(December 2018), 99–104. https://doi.org/10.1016/j.foodhyd.2018.12.010

Aman Mohammadi, M., Hosseini, S. M., & Yousefi, M. (2020). Application of electrospinning technique in development of intelligent food packaging: A short review of recent trends. In *Food Science and Nutrition* (Vol. 8, Issue 9, pp. 4656–4665). Wiley-Blackwell. https://doi.org/10.1002/fsn3.1781

Amna, R., Ali, K., Malik, M. I., & Shamsah, S. I. (2020). A brief review of electrospinning of polymer nanofibers: History and main applications. *Journal of New Materials for Electrochemical Systems*, *23*(3), 151–163. https://doi.org/10.14447/jnmes.v23i3.a01

Araghi, M., Moslehi, Z., Nafchi, A. M., Mostahsan, A., Salamat, N., & Garmakhany, A. D. (2015). Cold water fish gelatin modification by a natural

phenolic cross-linker (ferulic acid and caffeic acid). *Food Science and Nutrition*, *3*(5), 370–375. https://doi.org/10.1002/fsn3.230

Arkoun, M., Holley, R. A., & Heuzey, M. C. (2018). *Chitosan - based nanofibers as bioactive meat packaging materials*. *May 2017*, 185–195. https://doi.org/10.1002/pts.2366

Ashraf, R., Sofi, H. S., Malik, A., Beigh, M. A., Hamid, R., & Sheikh, F. A. (2019). Recent Trends in the Fabrication of Starch Nanofibers: Electrospinning and Non-electrospinning Routes and Their Applications in Biotechnology. *Applied Biochemistry and Biotechnology*, *187*(1), 47–74. https://doi.org/10.1007/s12010-018-2797-0

Aslaner, G., Sumnu, G., & Sahin, S. (2021). Encapsulation of Grape Seed Extract in Rye Flour and Whey Protein–Based Electrospun Nanofibers. *Food and Bioprocess Technology*, *14*(6), 1118–1131. https://doi.org/10.1007/s11947-021-02627-w

Aydogdu, A., Kirtil, E., Sumnu, G., Oztop, M. H., & Aydogdu, Y. (2018). Utilization of lentil flour as a biopolymer source for the development of edible films. *Journal of Applied Polymer Science*, *135*(23). https://doi.org/10.1002/app.46356

Aydogdu, A., Sumnu, G., & Sahin, S. (2018). A novel electrospun hydroxypropyl methylcellulose/polyethylene oxide blend nanofibers: Morphology and physicochemical properties. *Carbohydrate Polymers*, *181*, 234–246. https://doi.org/10.1016/J.CARBPOL.2017.10.071

Aydogdu, A., Sumnu, G., & Sahin, S. (2019). Fabrication of gallic acid loaded Hydroxypropyl methylcellulose nanofibers by electrospinning technique as active packaging material. *Carbohydrate Polymers*, *208*, 241–250. https://doi.org/10.1016/j.carbpol.2018.12.065

Aydogdu, A., Yildiz, E., Aydogdu, Y., Sumnu, G., Sahin, S., & Ayhan, Z. (2019). Food Hydrocolloids Enhancing oxidative stability of walnuts by using gallic

acid loaded lentil flour based electrospun nanofibers as active packaging material. *Food Hydrocolloids*, *95*(April), 245–255. https://doi.org/10.1016/j.foodhyd.2019.04.020

Beikzadeh, S., Akbarinejad, A., Swift, S., Perera, J., Kilmartin, P. A., & Travas-Sejdic, J. (2020). Cellulose acetate electrospun nanofibers encapsulating Lemon Myrtle essential oil as active agent with potent and sustainable antimicrobial activity. *Reactive and Functional Polymers*, *157*. https://doi.org/10.1016/j.reactfunctpolym.2020.104769

Benbettaieb, N., Nyagaya, J., Seuvre, A. M., & Debeaufort, F. (2018). Antioxidant Activity and Release Kinetics of Caffeic and p-Coumaric Acids from Hydrocolloid-Based Active Films for Healthy Packaged Food. *Journal of Agricultural and Food Chemistry*, *66*(26), 6906–6916. https://doi.org/10.1021/acs.jafc.8b01846

Benbettaïeb, N., Tanner, C., Cayot, P., Karbowiak, T., & Debeaufort, F. (2018). Impact of functional properties and release kinetics on antioxidant activity of biopolymer active films and coatings. *Food Chemistry*, *242*(September 2017), 369–377. https://doi.org/10.1016/j.foodchem.2017.09.065

Castro Coelho, S., Nogueiro Estevinho, B., & Rocha, F. (2021). Encapsulation in food industry with emerging electrohydrodynamic techniques: Electrospinning and electrospraying – A review. In *Food Chemistry* (Vol. 339). Elsevier Ltd. https://doi.org/10.1016/j.foodchem.2020.127850

Celebioglu, A., & Uyar, T. (2020). Design of polymer-free Vitamin-A acetate/cyclodextrin nanofibrous webs: Antioxidant and fast-dissolving properties. *Food and Function*, *11*(9), 7626–7637. https://doi.org/10.1039/d0fo01776k

Chen, H., Wang, J., Cheng, Y., Wang, C., Liu, H., Bian, H., Pan, Y., Sun, J., & Han, W. (2019). Application of Protein-Based Films and Coatings for Food

Packaging: A Review. *Polymers*, *11*(12), 2039. https://doi.org/10.3390/polym11122039

Chen, J. H., & Ho, C.-T. (1997). *Antioxidant Activities of Caffeic Acid and Its Related Hydroxycinnamic Acid Compounds*.

Colín-Orozco, J., Zapata-Torres, M., Rodríguez-Gattorno, G., & Pedroza-Islas, R. (2015). Properties of Poly (ethylene oxide)/ whey Protein Isolate Nanofibers Prepared by Electrospinning. *Food Biophysics*, *10*(2), 134–144. https://doi.org/10.1007/S11483-014-9372-1

da Silva Filipini, G., Romani, V. P., & Guimarães Martins, V. (2020). Biodegradable and active-intelligent films based on methylcellulose and jambolão (Syzygium cumini) skins extract for food packaging. *Food Hydrocolloids*, *109*(May). https://doi.org/10.1016/j.foodhyd.2020.106139

Deitzel, J. M., Kleinmeyer, J., Harris, D., & Tan, N. C. B. (n.d.). *The effect of processing variables on the morphology of electrospun nanofibers and textiles*. www.elsevier.nl/locate/polymer

Drosou, C., Krokida, M., & Biliaderis, C. G. (2018). Composite pullulan-whey protein nanofibers made by electrospinning: Impact of process parameters on fiber morphology and physical properties. *Food Hydrocolloids*, *77*, 726–735. https://doi.org/10.1016/j.foodhyd.2017.11.014

Fathi, M., Mirlohi, M., Varshosaz, J., & Madani, G. (2013). Novel Caffeic Acid Nanocarrier: Production, Characterization, and Release Modeling. *Journal of Nanomaterials*, *2013*. https://doi.org/10.1155/2013/434632

Gaikwad, K. K., Singh, S., & Lee, Y. S. (2019). Antimicrobial and improved barrier properties of natural phenolic compound-coated polymeric films for active packaging applications. *Journal of Coatings Technology and Research*, *16*(1), 147–157. https://doi.org/10.1007/s11998-018-0109-9

Guan, X., Li, L., Li, S., Liu, J., & Huang, K. (2020). A food-grade continuous electrospun fiber of hordein/chitosan with water resistance. *Food Bioscience*, *37*. https://doi.org/10.1016/j.fbio.2020.100687

Haider, A., Haider, S., & Kang, I. K. (2018). A comprehensive review summarizing the effect of electrospinning parameters and potential applications of nanofibers in biomedical and biotechnology. In *Arabian Journal of Chemistry* (Vol. 11, Issue 8, pp. 1165–1188). Elsevier B.V. https://doi.org/10.1016/j.arabjc.2015.11.015

Hernández-Fernández, J., Rayón, E., López, J., & Arrieta, M. P. (2019). Enhancing the Thermal Stability of Polypropylene by Blending with Low Amounts of Natural Antioxidants. *Macromolecular Materials and Engineering*, *304*(11), 1–13. https://doi.org/10.1002/mame.201900379

Ignatova, M. G., Manolova, N. E., Rashkov, I. B., Markova, N. D., Toshkova, R. A., Georgieva, A. K., & Nikolova, E. B. (2016). Poly(3-hydroxybutyrate)/caffeic acid electrospun fibrous materials coated with polyelectrolyte complex and their antibacterial activity and in vitro antitumor effect against HeLa cells. *Materials Science and Engineering C*, *65*, 379–392. https://doi.org/10.1016/j.msec.2016.04.060

Ignatova, M., Manolova, N., Rashkov, I., & Markova, N. (2018). Antibacterial and antioxidant electrospun materials from poly(3-hydroxybutyrate) and polyvinylpyrrolidone containing caffeic acid phenethyl ester – “in” and “on” strategies for enhanced solubility. *International Journal of Pharmaceutics*, *545*(1–2), 342–356. https://doi.org/10.1016/j.ijpharm.2018.05.013

Insaward, A., Duangmal, K., & Mahawanich, T. (2015). Mechanical, Optical, and Barrier Properties of Soy Protein Film As Affected by Phenolic Acid Addition. *Journal of Agricultural and Food Chemistry*, *63*(43), 9421–9426. https://doi.org/10.1021/jf504016m

Ivanković, A., Talić, S., & Lasić, M. (2017). *BIODEGRADABLE PACKAGING IN THE FOOD INDUSTRY*. https://doi.org/10.2376/0003-925X-68-26

Kumar, A., & Sinha-Ray, S. (2018). A review on biopolymer-based fibers via electrospinning and solution blowing and their applications. In *Fibers* (Vol. 6, Issue 3). MDPI Multidisciplinary Digital Publishing Institute. https://doi.org/10.3390/fib6030045

Kuntzler, S. G., Costa, J. A. V., & Morais, M. G. de. (2018). Development of electrospun nanofibers containing chitosan/PEO blend and phenolic compounds with antibacterial activity. *International Journal of Biological Macromolecules*, *117*, 800–806. https://doi.org/10.1016/j.ijbiomac.2018.05.224

Kutzli, I., Gibis, M., Baier, S. K., & Weiss, J. (2019). Food Hydrocolloids Electrospinning of whey and soy protein mixed with maltodextrin – Influence of protein type and ratio on the production and morphology of fibers. *Food Hydrocolloids*, *93*(January), 206–214. https://doi.org/10.1016/j.foodhyd.2019.02.028

Li, Y., Zhu, J., Cheng, H., Li, G., Cho, H., Jiang, M., Gao, Q., & Zhang, X. (2021). Developments of Advanced Electrospinning Techniques: A Critical Review. In *Advanced Materials Technologies* (Vol. 6, Issue 11). John Wiley and Sons Inc. https://doi.org/10.1002/admt.202100410

Li, Z., & Wang, · Ce. (n.d.). *SPRINGER BRIEFS IN MATERIALS One-Dimensional Nanostructures Electrospinning Technique and Unique Nanofibers*. http://www.springer.com/series/10111

Liu, Y., Liang, X., Wang, S., Qin, W., & Zhang, Q. (2018). Electrospun antimicrobial polylactic acid/tea polyphenol nanofibers for food-packaging applications. *Polymers*, *10*(5). https://doi.org/10.3390/polym10050561

Luzi, F., Torre, L., & Puglia, D. (2020). Antioxidant Packaging Films Based on Ethylene Vinyl Alcohol Copolymer (EVOH) and Caffeic Acid. *Molecules*, *25*(17). https://doi.org/10.3390/molecules25173953

Medina Jaramillo, C., Gutiérrez, T. J., Goyanes, S., Bernal, C., & Famá, L. (2016). Biodegradability and plasticizing effect of yerba mate extract on cassava starch edible films. *Carbohydrate Polymers*, *151*, 150–159. https://doi.org/10.1016/j.carbpol.2016.05.025

Medina-Jaramillo, C., Ochoa-Yepes, O., Bernal, C., & Famá, L. (2017). Active and smart biodegradable packaging based on starch and natural extracts. *Carbohydrate Polymers*, *176*(August), 187–194. https://doi.org/10.1016/j.carbpol.2017.08.079

Mercante, L. A., Scagion, V. P., Migliorini, F. L., Mattoso, L. H. C., & Correa, D. S. (2017). Electrospinning-based (bio)sensors for food and agricultural applications: A review. In *TrAC - Trends in Analytical Chemistry* (Vol. 91, pp. 91–103). Elsevier B.V. https://doi.org/10.1016/j.trac.2017.04.004

Muthu, T. S., Kumar, K. S., Rajini, N., Siengchin, S., Ayrilmis, N., & Rajulu, A. V. (2019). A comprehensive review of electrospun nanofibers : Food and packaging perspective. *Composites Part B*, *175*(July), 107074. https://doi.org/10.1016/j.compositesb.2019.107074

Neo, Y. P., Ray, S., Jin, J., Gizdavic-Nikolaidis, M., Nieuwoudt, M. K., Liu, D., & Quek, S. Y. (2013). Encapsulation of food grade antioxidant in natural biopolymer by electrospinning technique: A physicochemical study based on zein-gallic acid system. *Food Chemistry*, *136*(2), 1013–1021. https://doi.org/10.1016/j.foodchem.2012.09.010

Nikbaht, M., Salehi, M., Rezayat, seyed mahdi, & Majidi, reza faridi. (2020). *Various parameters in the preparation of chitosan / polyethylene oxide electrospun nanofibers containing Aloe vera extract for medical applications*. *7*(1), 21–28. https://doi.org/10.22038/nmj.2020.07.03

Oguz, S., Tam, N., Aydogdu, A., Sumnu, G., & Sahin, S. (2018). Development of novel pea flour-based nanofibres by electrospinning method. *International Journal of Food Science and Technology*, *53*(5), 1269–1277. https://doi.org/10.1111/ijfs.13707

Okutan, N., Terzi, P., & Altay, F. (2014). Affecting parameters on electrospinning process and characterization of electrospun gelatin nanofibers. *Food Hydrocolloids*, *39*, 19–26. https://doi.org/10.1016/j.foodhyd.2013.12.022

Ouahioune, L. A., Wrona, M., Nerín, C., & Djenane, D. (2022). Novel active biopackaging incorporated with macerate of carob (Ceratonia siliqua L.) to extend shelf-life of stored Atlantic salmon fillets (Salmo salar L.). *LWT*, *156*. https://doi.org/10.1016/j.lwt.2021.113015

Papaefstathiou, E., Agapiou, A., Giannopoulos, S., & Kokkinofta, R. (2018). Nutritional characterization of carobs and traditional carob products. *Food Science and Nutrition*, *6*(8), 2151–2161. https://doi.org/10.1002/fsn3.776

Pelipenko, J., Kristl, J., Janković, B., Baumgartner, S., & Kocbek, P. (2013). The impact of relative humidity during electrospinning on the morphology and mechanical properties of nanofibers. *International Journal of Pharmaceutics*, *456*(1), 125–134. https://doi.org/10.1016/j.ijpharm.2013.07.078

Pérez, M. J., Moreno, M. A., Martínez-Abad, A., Cattaneo, F., Zampini, C., Isla, M. I., López-Rubio, A., & Fabra, M. J. (2021). Interest of black carob extract for the development of active biopolymer films for cheese preservation. *Food Hydrocolloids*, *113*. https://doi.org/10.1016/j.foodhyd.2020.106436

Rangaraj, V. M., Rambabu, K., Banat, F., & Mittal, V. (2021). Natural antioxidants-based edible active food packaging: An overview of current advancements. In *Food Bioscience* (Vol. 43). Elsevier Ltd. https://doi.org/10.1016/j.fbio.2021.101251

Rani, P., Yu, X., Liu, H., Li, K., He, Y., Tian, H., & Kumar, R. (2021). Material, antibacterial and anticancer properties of natural polyphenols incorporated soy

protein isolate: A review. *European Polymer Journal*, *152*(April). https://doi.org/10.1016/j.eurpolymj.2021.110494

Rodsamran, P., & Sothornvit, R. (2019). Lime peel pectin integrated with coconut water and lime peel extract as a new bioactive film sachet to retard soybean oil oxidation. *Food Hydrocolloids*, *97*(June), 105173. https://doi.org/10.1016/j.foodhyd.2019.105173

Sanches-Silva, A., Costa, D., Albuquerque, T. G., Buonocore, G. G., Ramos, F., Castilho, M. C., Machado, A. V., & Costa, H. S. (2014). Trends in the use of natural antioxidants in active food packaging: a review. *Food Additives and Contaminants - Part A Chemistry, Analysis, Control, Exposure and Risk Assessment*, *31*(3), 374–395. https://doi.org/10.1080/19440049.2013.879215

Schiffman, J. D., & Schauer, C. L. (2008). A review: Electrospinning of biopolymer nanofibers and their applications. In *Polymer Reviews* (Vol. 48, Issue 2, pp. 317–352). https://doi.org/10.1080/15583720802022182

Shao, P., Niu, B., Chen, H., & Sun, P. (2018). Fabrication and characterization of tea polyphenols loaded pullulan-CMC electrospun nanofiber for fruit preservation. *International Journal of Biological Macromolecules*, *107*, 1908–1914. https://doi.org/10.1016/j.ijbiomac.2017.10.054

Singthong, J., Oonsivilai, R., Oonmetta-Aree, J., & Ningsanond, S. (2014). Bioactive compounds and encapsulation of Yanang (Tiliacora triandra) leaves. *African Journal of Traditional, Complementary, and Alternative Medicines : AJTCAM / African Networks on Ethnomedicines*, *11*(3), 76–84. https://doi.org/10.4314/ajtcam.v11i3.11

Sullivan, S. T., Tang, C., Kennedy, A., Talwar, S., & Khan, S. A. (2014). Food Hydrocolloids Electrospinning and heat treatment of whey protein nano fi bers. *Food Hydrocolloids*, *35*, 36–50. https://doi.org/10.1016/j.foodhyd.2013.07.023

Tam, N., Oguz, S., Aydogdu, A., Sumnu, G., & Sahin, S. (2017). Influence of solution properties and pH on the fabrication of electrospun lentil flour/HPMC blend nanofibers. *Food Research International*, *102*, 616–624. https://doi.org/10.1016/j.foodres.2017.09.049

Tatlisu, N. B., Yilmaz, M. T., & Arici, M. (2019). Fabrication and characterization of thymol-loaded nanofiber mats as a novel antimould surface material for coating cheese surface. *Food Packaging and Shelf Life*, *21*(March), 100347. https://doi.org/10.1016/j.fpsl.2019.100347

Thenmozhi, S., Dharmaraj, N., Kadirvelu, K., & Kim, H. Y. (2017). Electrospun nanofibers: New generation materials for advanced applications. In *Materials Science and Engineering B: Solid-State Materials for Advanced Technology* (Vol. 217, pp. 36–48). Elsevier Ltd. https://doi.org/10.1016/j.mseb.2017.01.001

Uyar, T., & Besenbacher, F. (2008). Electrospinning of uniform polystyrene fibers: The effect of solvent conductivity. *Polymer*, *49*(24), 5336–5343. https://doi.org/10.1016/j.polymer.2008.09.025

Uygun, E., Yildiz, E., Sumnu, G., & Sahin, S. (2020). *Microwave Pretreatment for the Improvement of Physicochemical Properties of Carob Flour and Rice Starch – Based Electrospun Nanofilms*. 838–850.

Valizadeh, A., & Farkhani, S. M. (2014). Electrospinning and electrospun nanofibres. *IET Nanobiotechnology*, *8*(2), 83–92. https://doi.org/10.1049/iet-nbt.2012.0040

Vega-Lugo, A. C., & Lim, L. T. (2012). Effects of poly(ethylene oxide) and pH on the electrospinning of whey protein isolate. *Journal of Polymer Science, Part B: Polymer Physics*, *50*(16), 1188–1197. https://doi.org/10.1002/polb.23106

Vilchez, A., Acevedo, F., Cea, M., Seeger, M., & Navia, R. (2020). Applications of electrospun nanofibers with antioxidant properties: A review. *Nanomaterials*, *10*(1), 1–25. https://doi.org/10.3390/nano10010175

Wang, A., Leible, M., Lin, J., Weiss, J., & Zhong, Q. (2020). Caffeic Acid Phenethyl Ester Loaded in Skim Milk Microcapsules: Physicochemical Properties and Enhanced in Vitro Bioaccessibility and Bioactivity against Colon Cancer Cells. *Journal of Agricultural and Food Chemistry*, *68*(50), 14978–14987. https://doi.org/10.1021/acs.jafc.0c05143

Wen, P., Zong, M. H., Linhardt, R. J., Feng, K., & Wu, H. (2017). Electrospinning: A novel nano-encapsulation approach for bioactive compounds. In *Trends in Food Science and Technology* (Vol. 70, pp. 56–68). Elsevier Ltd. https://doi.org/10.1016/j.tifs.2017.10.009

Wilk, S., & Benko, A. (2021). Advances in fabricating the electrospun biopolymer-based biomaterials. *Journal of Functional Biomaterials*, *12*(2). https://doi.org/10.3390/jfb12020026

Woranuch, S., Pangon, A., Puagsuntia, K., Subjalearndee, N., & Intasanta, V. (2017). Rice flour-based nanostructures via a water-based system: transformation from powder to electrospun nanofibers under hydrogen-bonding induced viscosity, crystallinity and improved mechanical property. *RSC Advances*, *7*(32), 19960–19966. https://doi.org/10.1039/c7ra01485f

Wrona, M., Nerín, C., Alfonso, M. J., & Caballero, M. Á. (2017). Antioxidant packaging with encapsulated green tea for fresh minced meat. *Innovative Food Science and Emerging Technologies*, *41*(November 2016), 307–313. https://doi.org/10.1016/j.ifset.2017.04.001

Yildiz, E., Sumnu, G., & Kahyaoglu, L. N. (2021). Monitoring freshness of chicken breast by using natural halochromic curcumin loaded chitosan/PEO nanofibers as an intelligent package. *International Journal of Biological Macromolecules*, *170*, 437–446. https://doi.org/10.1016/j.ijbiomac.2020.12.160

Youssef, M. K. E., El-Manfaloty, M. M., & Ali, H. M. (2013). Assessment of proximate chemical composition, nutritional status, fatty acid composition and

phenolic compounds of carob (Ceratonia siliqua L.). *Food and Public Health*, *3*(6), 304–308. https://doi.org/10.5923/j.fph.20130306.06

Yu, S. H., Hsieh, H. Y., Pang, J. C., Tang, D. W., Shih, C. M., Tsai, M. L., Tsai, Y. C., & Mi, F. L. (2013). Active films from water-soluble chitosan/cellulose composites incorporating releasable caffeic acid for inhibition of lipid oxidation in fish oil emulsions. *Food Hydrocolloids*. https://doi.org/10.1016/j.foodhyd.2012.11.036

Zargham, S., Bazgir, S., Tavakoli, A., Rashidi, A. S., & Damerchely, R. (n.d.). *The Effect of Flow Rate on Morphology and Deposition Area of Electrospun Nylon 6 Nanofiber* (Vol. 7). http://www.jeffjournal.org

Zhang, C., Li, Y., Wang, P., & Zhang, H. (2020). Electrospinning of nanofibers: Potentials and perspectives for active food packaging. *Comprehensive Reviews in Food Science and Food Safety*, *June 2019*, 479–502. https://doi.org/10.1111/1541-4337.12536

Zhong, J., Mohan, S. D., Bell, A., Terry, A., Mitchell, G. R., & Davis, F. J. (2018). Electrospinning of food-grade nanofibres from whey protein. *International Journal of Biological Macromolecules*, *113*, 764–773. https://doi.org/10.1016/j.ijbiomac.2018.02.113

Zhu, B. J., Zayed, M. Z., Zhu, H. X., Zhao, J., & Li, S. P. (2019). Functional polysaccharides of carob fruit : a review. *Chinese Medicine*, 1–10. https://doi.org/10.1186/s13020-019-0261-x

APPENDICES

A. Statistical Analysis

Table A.1 One way Analysis of Variance (ANOVA) and Tukey's comparison test for consistency index (k) values of solutions containing different amount of WPC and CA

One-way ANOVA: k versus Solution

Method

Null hypothesis	All means are equal
Alternative hypothesis	Not all means are equal
Significance level	α = 0,05

Equal variances were assumed for the analysis.

Factor Information

Factor	Levels	Values
Solution	4	3C1W, 3C3W, 3C3W1CA, C3W10CA

Analysis of Variance

Source	DF	Seq SS	Adj MS	F-value	P-value
Solution	3	0,081606	0,027202	142,65	0,000
Error	4	0,000763	0,000191		
Total	7	0,082368			

Model Summary

S	R-sq	R-sq(adj)	R-sq(pred)
0,0138089	99,07%	98,38%	96,30%

Means

Solution	N	Mean	StDev	95% CI
3C1W	2	0,3862	0,0198	(0,3591; 0,4133)
3C3W	2	0,54519	0,01230	(0,51808;0,57230)
3C3W1CA	2	0,4507	0,0147	(0,4236; 0,4778)
3C3W10CA	2	0,26742	0,00172	(0,24031;0,29453)

Tukey Pairwise Comparisons

Grouping Information Using the Tukey Method and 95% Confidence

Solution	N	Mean	Grouping			
3C3W	2	0,54519	A			
3C3W1CA	2	0,4507		B		
3C1W	2	0,3862			C	
3C3W10CA	2	0,26742				D

Means that do not share a letter are significantly different.

Table A.2 One way Analysis of Variance (ANOVA) and Tukey's comparison test for flow behavior index (n) values of solutions containing different amount of WPC and CA

One-way ANOVA: n versus Solution

Method

Null hypothesis	All means are equal
Alternative hypothesis	Not all means are equal
Significance level	α = 0,05

Equal variances were assumed for the analysis.

Factor Information

Factor	Levels	Values
Solution	4	3C1W, 3C3W, 3C3W1CA,3C3W10CA

Analysis of Variance

Source	DF	Adj SS	Adj MS	F-value	P-value
solution	3	0,000582	0,000194	2,02	0,253
Error	4	0,000384	0,000096		
Total	7	0,000966			

Model Summary

S	R-sq	R-sq(adj)	R-sq(pred)
0,0097929	60,27%	30,48%	0,00%

Means

Solution	N	Mean	StDev	95% CI
3C1W	2	0,912100	0,001273	(0,892874; 0,931326)
3C3W	2	0,91240	0,00863	(0,89317;0,93163)
3C3W1CA	2	0,921450	0,000212	(0,902224; 0,940676)
3C3W10CA	2	0,9330	0,0175	(0,9138; 0,9522)

Tukey Pairwise Comparisons

Grouping Information Using the Tukey Method and 95% Confidence

Solution	N	Mean	Grouping
3C3W	2	0,9330	A
3C3W1CA	2	0,921450	A
3C1W	2	0,91240	A
3C3W10CA	2	0,912100	A

Means that do not share a letter are significantly different.

Table A.3 One way Analysis of Variance (ANOVA) and Tukey's comparison test for electrical conductivity values of solutions containing different amount of WPC and CA

One-way ANOVA: Electrical conductivity versus Solution

Method

Null hypothesis	All means are equal
Alternative hypothesis	Not all means are equal
Significance level	α = 0,05

Equal variances were assumed for the analysis.

Factor Information

Factor	Levels	Values
Solution	4	3C1W; 3C3W; 3C3W1CA; 3C3W10CA

Analysis of Variance

Source	DF	Adj SS	Adj MS	F-Value	P-Value
Solution	3	3,55004	1,18335	291,29	0,000
Error	4	0,01625	0,00406		
Total	7	3,56629			

Model Summary

S	R-sq	R-sq(adj)	R-sq(pred)
0,0637377	99,54%	99,20%	98,18%

Means

Solution	N	Mean	StDev	95% CI
3C1W	2	4,0300	0,0283	(3,9049; 4,1551)
3C3W	2	4,1000	0,0141	(3,9749; 4,2251)
3C3W1CA	2	4,7800	0,0283	(4,6549; 4,9051)
3C3W10CA	2	5,6850	0,1202	(5,5599; 5,8101)

Pooled StDev = 0,0637377

Tukey Pairwise Comparisons

Grouping Information Using the Tukey Method and 95% Confidence

Solution	N	Mean	Grouping		
3C3W10CA	2	5,6850	A		
3C3W1CA	2	4,7800		B	
3C3W	2	4,1000			C
3C1W	2	4,0300			C

Means that do not share a letter are significantly different.

Table A.4 One way Analysis of Variance (ANOVA) and Tukey's comparison test for average fiber diameters of nanofibers containing different amount of WPC and CA

One-way ANOVA: Diameter versus Film

Method

Null hypothesis	All means are equal
Alternative hypothesis	Not all means are equal
Significance level	α = 0,05

Equal variances were assumed for the analysis.

Factor Information

Factor	Levels	Values
Film	4	3C1W; 3C3W; 3C3W1CA; 3C3W10CA

Analysis of Variance

Source	DF	Adj SS	Adj MS	F-Value	P-Value
Film	3	421988	140663	37,77	0,000
Error	396	1474820	3724		
Total	399	1896808			

Model Summary

S	R-sq	R-sq(adj)	R-sq(pred)
61,0270	22,25%	21,66%	20,67%

Means

Film	N	Mean	StDev	95% CI
3C1W	100	241,91	56,38	(229,91; 253,91)
3C3W	100	309,58	70,28	(297,58; 321,58)
3C3W1CA	100	257,20	66,34	(245,20; 269,20)
3C3W10CA	100	221,94	48,77	(209,94; 233,94)

Pooled StDev = 61,0270

Tukey Pairwise Comparisons

Grouping Information Using the Tukey Method and 95% Confidence

Film	N	Mean	Grouping	
3C3W	100	309,58	A	
3C3W1CA	100	257,20	B	
3C1W	100	241,91	B	C
3C3W10CA	100	221,94		C

Means that do not share a letter are significantly different.

Table A.5 One way Analysis of Variance (ANOVA) and Tukey's comparison test for melting temperatures (T_m) of nanofibers containing different amount of WPC and CA

One-way ANOVA: Tm versus Film

Method

Null hypothesis	All means are equal
Alternative hypothesis	Not all means are equal
Significance level	$\alpha = 0,05$

Equal variances were assumed for the analysis.

Factor Information

Factor	Levels	Values
Film	4	3C1W, 3C3W, 3C3W10CA, 3C3W1CA

Analysis of Variance

Source	DF	Adj SS	Adj MS	F-Value
Film	3	12.1978	4.06593	43.49
Error	4	0.374	0.0935	
Total	7	12.5718		

Model Summary

S	R-sq	R-sq(adj)	R-sq(pred)
0.305778	97.03%	94.79%	88.10%

Means

Film	N	Mean	StDev	95% CI
3C1W	2	63.9	0.141	(63.300, 64.500)
3C3W	2	60.92	0.1131	(60.3197, 61.5203)
3C3W10CA	2	62.71	0.58	(62.110, 63.310)
3C3W1CA	2	61.05	0.0707	(60.4497, 61.6503)

Tukey Pairwise Comparisons

Grouping Information Using the Tukey Method and 95% Confidence

Film	N	Mean	Grouping	
3C1W	2	63.9	A	
3C3W10CA	2	62.71	A	
3C3W1CA	2	61.05		B
3C3W	2	60.92		B

Means that do not share a letter are significantly different.

Table A.6 One way Analysis of Variance (ANOVA) and Tukey's comparison test for ΔH of nanofibers containing different amount of WPC and CA

One-way ANOVA: ΔH versus Film

Method

Null hypothesis	All means are equal
Alternative hypothesis	Not all means are equal
Significance level	α = 0,05

Equal variances were assumed for the analysis.

Factor Information

Factor	Levels	Values
Film	4	3C1W, 3C3W, 3C3W10CA, 3C3W1CA

Analysis of Variance

Source	DF	Adj SS	Adj MS	F-Value	P-Value
Film	3	241.088	80.3626	615.57	0
Error	4	0.522	0.1305		
Total	7	241.61			

Model Summary

S	R-sq	R-sq(adj)	R-sq(pred)
0.361317	99.78%	99.62%	99.14%

Means

Film	N	Mean	StDev	95% CI
3C1W	2	40.89	0.156	(40.181, 41.599)
3C3W	2	36.47	0.665	(35.761, 37.179)
3C3W10CA	2	28.16	0.226	(27.451, 28.869)
3C3W1CA	2	28.15	0.0707	(27.4406, 28.8594)

Tukey Pairwise Comparisons

Grouping Information Using the Tukey Method and 95% Confidence

Film	N	Mean	Grouping		
3C1W	2	40.89	A		
3C3W	2	36.47		B	
3C3W10CA	2	28.16			C
3C3W1CA	2	28.15			C

Means that do not share a letter are significantly different.

Table A.7 One way Analysis of Variance (ANOVA) and Tukey's comparison test for glass transition temperatures (T_g) of nanofibers containing different amount of WPC and CA

One-way ANOVA: Tg versus Film

Method

Null hypothesis	All means are equal
Alternative hypothesis	Not all means are equal
Significance level	α = 0,05

Equal variances were assumed for the analysis.

Factor Information

Factor	Levels	Values
Film	4	3C1W, 3C3W, 3C3W10CA, 3C3W1CA

Analysis of Variance

Source	DF	Adj SS	Adj MS	F-Value	P-Value
Film	3	27.634	9.2113	28.26	0.004
Error	4	1.304	0.3259		
Total	7	28.937			

Model Summary

S	R-sq	R-sq(adj)	R-sq(pred)
0.570877	95.50%	92.12%	81.98%

Means

Film	N	Mean	StDev	95% CI
3C1W	2	-5.28	0.877	(-6.401, -4.159)
3C3W	2	-9.36	0.509	(-10.481, -8.239)
3C3W10CA	2	-9.47	0.24	(-10.591, -8.349)
3C3W1CA	2	-9.83	0.467	(-10.951, -8.709)

Tukey Pairwise Comparisons

Grouping Information Using the Tukey Method and 95% Confidence

Solution	N	Mean	Grouping	
3C1W	2	-5.28	A	
3C3W	2	-9.36		B

3C3W10CA	2	-9.47	B
3C3W1CA	2	-9.83	B

Table A.8 One way Analysis of Variance (ANOVA) and Tukey's comparison test for water vapor permeability (WVP) of nanofibers containing different amount of WPC and CA

One-way ANOVA: WVP versus Film

Method

Null hypothesis	All means are equal
Alternative hypothesis	Not all means are equal
Significance level	α = 0,05

Equal variances were assumed for the analysis.

Means

Film	N	Mean	StDev	95% CI
3C1W	2	0,000000	0,0000000000212132	(0,000000; 0,000000)
3C3W	2	0,000000	0,0000000000141421	(0,000000; 0,000000)
3C3W10CA	2	0,000000	0,0000000000098995	(0,000000; 0,000000)
3C3W1CA	2	0,000000	0,0000000000077782	(0,000000; 0,000000)

Pooled StDev = 1,421707E-11

Tukey Pairwise Comparisons

Grouping Information Using the Tukey Method and 95% Confidence

Film	N	Mean	Grouping		
3C1W	2	0,0000000002950000	A		
3C3W1CA	2	0,0000000002055000		B	
3C3W10CA	2	0,0000000001910000		B	C
3C3W	2	0,0000000001380000			C

Means that do not share a letter are significantly different.

Table A.9 One way Analysis of Variance (ANOVA) and Tukey's comparison test for antioxidant activity (AA) of nanofibers containing different amount CA

One-way ANOVA: AA versus Film

Method

Null hypothesis	All means are equal
Alternative hypothesis	Not all means are equal
Significance level	α = 0,05

Equal variances were assumed for the analysis.

Factor Information

Factor	Levels	Values
Film	3	Control; 3C3W1CA; 3C3W10CA

Analysis of Variance

Source	DF	Adj SS	Adj MS	F-Value	P-Value
Film	2	8799,72	4399,86	6993,72	0,000
Error	3	1,89	0,63		
Total	5	8801,61			

Model Summary

S	R-sq	R-sq(adj)	R-sq(pred)
0,793169	99,98%	99,96%	99,91%

Means

Film	N	Mean	StDev	95% CI
Control	2	0,8500	0,0283	(-0,9349; 2,6349)
3C3W1CA	2	31,471	0,687	(29,686; 33,256)
3C3W10CA	2	92,950	1,189	(91,165; 94,734)

Pooled StDev = 0,793169

Tukey Pairwise Comparisons

Grouping Information Using the Tukey Method and 95% Confidence

Film	N	Mean	Grouping		
3C3W10CA	2	92,950	A		
3C3W1CA	2	31,471		B	
Control	2	0,8500			C

Means that do not share a letter are significantly different.

Table A.10 One way Analysis of Variance (ANOVA) and Tukey's comparison test for loading efficiency (LE) of nanofibers containing different amount CA

One-way ANOVA: LE versus Film

Method

Null hypothesis	All means are equal
Alternative hypothesis	Not all means are equal
Significance level	α = 0,05

Equal variances were assumed for the analysis.

Factor Information

Factor	Levels	Values
Film	2	3C3W1CA; 3C3W10CA

Analysis of Variance

Source	DF	Adj SS	Adj MS	F-Value	P-Value
Film	1	307,657	307,657	138,69	0,007
Error	2	4,437	2,218		
Total	3	312,094			

Model Summary

S	R-sq	R-sq(adj)	R-sq(pred)
1,48940	98,58%	97,87%	94,31%

Means

Film	N	Mean	StDev	95% CI
3C3W1CA	2	76,410	1,246	(71,878; 80,941)
3C3W10CA	2	93,95	1,70	(89,42; 98,48)

Pooled StDev = 1,48940

Tukey Pairwise Comparisons

Grouping Information Using the Tukey Method and 95% Confidence

Film	N	Mean	Grouping
3C3W10CA	2	93,95	A
3C3W1CA	2	76,410	B

Means that do not share a letter are significantly different.